

This is the accepted author manuscript of the publication

Synthesis and *in vitro* characterization of novel fluorinated derivatives of the translocator protein 18 kDa ligand CfO-DPA-714

Fanny Cacheux,^{a,b,#} Vincent Médran-Navarrete,^{a,b,#} Frédéric Dollé,^{a,b} Frank Marguet,^c Frédéric Puech,^c
Annelaure Damont.^{a,b}

^a*CEA, I2BM, Service Hospitalier Frédéric Joliot, Orsay, France.*

^b*Inserm / CEA / Université Paris Sud, UMR 1023 – ERL 9218 CNRS, IMIV, Université Paris-Saclay, Orsay, France.*

^c*Sanofi, LGCR ChemBio, Chilly-Mazarin, France.*

[#] contributed equally to this work

Corresponding Author

Annelaure Damont. CEA, I2BM, Service Hospitalier Frédéric Joliot, 4 Place du Général Leclerc, 91400 Orsay, France.

E-mail address: annelaure.damont@cea.fr

published in Eur J Med Chem. 2016 Sep 9;125:346-359.

doi: 10.1016/j.ejmech.2016.09.025

The final publication is available at

<http://www.sciencedirect.com/science/article/pii/S0223523416307553>

© 2016. This manuscript version is made available under the CC-BY-NC-ND 4.0 license

<http://creativecommons.org/licenses/by-nc-nd/4.0/>

Abstract

The translocator protein 18 kDa (TSPO) is today a validated target for a number of therapeutic applications, but also a well-recognized diagnostic / imaging biomarker for the evaluation of inflammatory related-disease state and progression, prompting the development of specific and dedicated TSPO ligands worldwide. For this purpose, pyrazolo[1,5-a]pyrimidine acetamides constitute a unique class of high affinity and selectivity TSPO ligands; it includes DPA-714, a fluorine-containing derivative that has also been labelled with the positron-emitter fluorine-18, and is nowadays widely used as a Positron Emission Tomography imaging probe. Recently, to prevent defluorination issues encountered *in vivo* with this tracer, a first series of analogues was reported where the oxygen atom bridging the phenyl ring of the core structure and the fluorinated moiety was replaced with a more robust linkage. Among this new series, CfO-DPA-714 was discovered as a highly promising TSPO ligand. Herein, a novel series of fluorinated analogues of the latter molecule were synthesized and *in vitro* characterized, where the pharmacomodulation at the amide position of the molecule was explored. Thirteen compounds were thus prepared from a common key-ester intermediate (synthesized in 7 steps from 4-iodobenzoate – 11 % overall yield) and a set of commercially available amines and obtained with moderate to good yields (23 to 81 %) and high purities (> 95 %). With one exception, all derivatives displayed nanomolar to subnanomolar affinity for the TSPO and also high selectivity versus the CBR (K_i (CBR) / K_i (TSPO) > 10^3). Within this series, three compounds showed better K_i values (0.25, 0.26 and 0.30 nM) than that of DPA-714 (0.91 nM) and CfO-DPA-714 (0.37 nM), and favorable lipophilicity for brain penetration ($3.6 < \log D_{7.4} < 4.4$). Among these three compounds, the *N*-methyl-*N*-propyl amide analogue (**9**) exhibited similar metabolic stability when compared to CfO-DPA-714 in mouse, rat and human microsomes. Therefore, the latter compound stands out as a promising candidate for drug development or for use as a PET probe, once fluorine-18-labelled, for *in vivo* neuroinflammation imaging.

Keywords:

TSPO 18 kDa

Pyrazolo[1,5-a]pyrimidine acetamides

CfO-DPA-714

Positron Emission Tomography

Neuroinflammation

1. Introduction

The Translocator protein (TSPO) 18 kDa, formerly known as the peripheral benzodiazepine receptor (PBR), is a highly lipophilic tryptophan-rich protein (169 amino acids) with five transmembrane α -helices domain and whose sequence is highly conserved among organisms [1]. Combined with a 32 kDa voltage dependent anion channel (VDAC) and a 30 kDa adenine nucleoside carrier (ANC), TSPO forms the mitochondrial permeability transition pore (MPTP), a complex primary located on the outer mitochondrial membrane [2]. TSPO is expressed predominantly in steroid-synthesizing tissues, including the brain, and the most characterized function of this protein is the translocation of cholesterol from the outer to the inner mitochondrial membrane, which is the rate-limiting step in the synthesis of steroids and neurosteroids [3]. TSPO is also implicated in other biochemical processes including cell proliferation and apoptosis. In the healthy brain, baseline TSPO expression levels remain low, but increased TSPO expression has been associated with activated states of microglia and especially in areas damaged by neurodegenerative diseases (Alzheimer's disease and other dementias, Parkinson's disease, multiple sclerosis, stroke) [4]. TSPO is also overexpressed in certain cancers, such as glioma, where the protein levels directly correlate with aggressive metastatic behaviours [5,6], and in activated macrophages, involved for example in peripheral inflammatory diseases (inflammatory bowel disease and rheumatoid arthritis) [1].

As such, the TSPO is today a validated target for a number of therapeutic applications for neurological but also psychiatric disorders (neuronal viability, regenerative processes and neuroinflammatory responses) [4,7]. It is also becoming an attractive target for cancer chemotherapy, where the altered regulation of numerous cellular processes and especially those associated with mitochondria and cholesterol transport, are partially responsible for the unrestrained growth of tumourigenic tissues [5,6]. Moreover, TSPO is a well-recognized imaging biomarker for the evaluation of inflammatory related-disease state and progression [8,9], further prompting the development of specific and dedicated ligands worldwide, for dual therapeutic / diagnostic issues, but with today a strong emphasis towards imaging probes [10–14].

Several classes of TSPO ligands have been reported to date, leading to an impressive list of compounds that starts with the isoquinoline carboxamide PK11195 (Figure 1) [11]. This compound is not only the first non-benzodiazepine reported and developed (Pharmuka laboratories) TSPO ligand, showing a high affinity and selectivity in all species, but evermore the radioligand of reference for binding and autoradiographic studies worldwide once labelled with tritium ($[^3\text{H}]$ PK11195). Additionally, labelled with the positron-emitter carbon-11, $[^{11}\text{C}]$ PK11195 has been and is still widely used in (non-invasive) Positron Emission Tomography (PET) imaging studies, both at preclinical and clinical stages, despite the short-half-life of the radioisotope used ($T_{1/2}$ 20.38 min) [15]. TSPO ligands also include pyridazino[4,5-*b*]indole acetamides, and notably SSR180575 (Sanofi-Synthélabo) as neuroprotective drug with particular mitochondria-rescuing properties [16,17]. Labelled with carbon-11 [18], $[^{11}\text{C}]$ SSR180575 has recently demonstrated its potential to image neuroinflammatory processes with PET in both rodent [19] and non-human-primate [20] models of neurodegenerative diseases. Furthermore, derivatives of this class, featuring a fluorine atom in their structure that could be easily labelled by the longer half-life positron-emitter fluorine-18 ($T_{1/2}$ 109.8 min), have recently been reported [21,22].

Another class of particularly interesting TSPO ligands gathers imidazo[1,2-*a*]pyridine acetamides, a series that includes two well-known drugs: Zolpidem (Stilnox[®] - Sanofi, for the treatment of insomnia) and Alpidem (Ananxyl[®] - Synthélabo, as anxiolytic). This series also contains, as PET-imaging probes, $[^{11}\text{C}]$ CLINME [23,24] and $[^{18}\text{F}]$ PBR111 [25–29], and as Single Photon Emission Tomography (SPET) probe, the iodine-123-labelled derivative $[^{123}\text{I}]$ CLINDE [30–33]. $[^{123}\text{I}]$ CLINDE and $[^{18}\text{F}]$ PBR111 are today both engaged in humans studies [34,35], respectively with indications for multiform glioblastoma [36] and microglial activation imaging in patients with multiple sclerosis [37].

Pyrazolo[1,5-*a*]pyrimidine acetamides are azaisosters of the previous series, originally reported by the universities of Firenze and Pisa [38] with, as first developed lead compound, the *para*-tolyl derivative Me-DPA (Figure 1). Today, numerous alkoxy derivatives showing subnanomolar to picomolar affinities for the TSPO have been reported [39,40], with several compounds also demonstrating potent steroidogenic activities [41]. Of particular interest for diagnostic purposes, is the *para*-methoxy phenyl derivative DPA-713 and especially its fluorinated analogue, DPA-714. Labelled respectively with carbon-11 [42,43] and fluorine-18 [44–46], both radioligands showed improved PET imaging properties in rodent models of acute neuroinflammation, compared to [¹¹C]PK11195 [47–49]. [¹¹C]DPA-713 has also been recently engaged in clinical trials [50,51], and especially one with patients suffering from temporal lobe epilepsy [52]. On the other hand, [¹⁸F]DPA-714 is slowly but surely becoming “the” probe for microglia / macrophage activation imaging, thus dethroning the ligand of reference [¹¹C]PK11195. It has been validated in numerous rodent models of diseases such as acute focal or diffuse neuroinflammation [53,54], amyotrophic lateral sclerosis [55], subarachnoid hemorrhage [56], cerebral ischemia [57,58], peripheral and central cancers [59] including glioma [60], rheumatoid arthritis [61,62], and inflammatory bowel disease [63]. [¹⁸F]DPA-714 has also recently been characterized in a primate model of neuroinflammation [64] and engaged in a few first-in-man clinical trials [65–67]. It is also currently used in patients suffering from Alzheimer’s disease [68,69] and cerebral stroke [70].

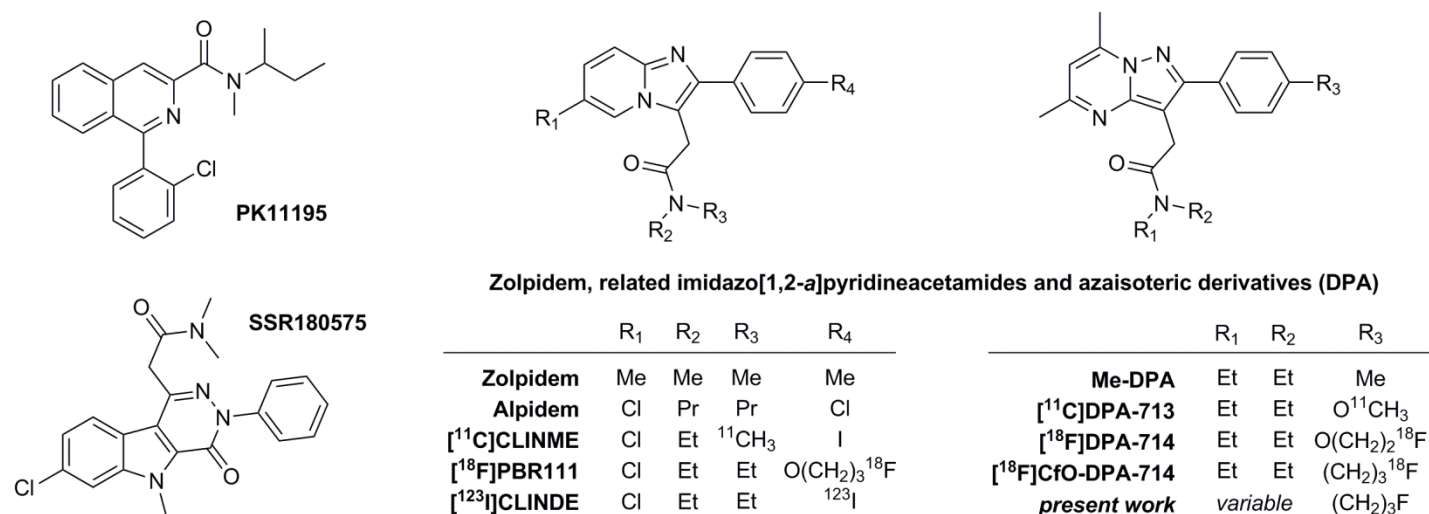


Figure 1. Representative examples of TSPO ligands: the isoquinoline carboxamide PK11195, the pyridazino[4,5-*b*]indole acetamide SSR180575, and selected imidazo[1,2-*a*]pyridine acetamides and pyrazolo[1,5-*a*]pyrimidine acetamides.

However, issues related to metabolism limit today the full potential of these series. Indeed, as first reported for imidazo[1,2-*a*]pyridine acetamide analogues, biotransformations that are mainly linked to cytochromes P450 3A4 and 2D6 expression and activity, lead to rapid *in vivo* elimination of the drug candidate or radiotracer. Metabolism includes hydroxylation at the methylaryl positions (e.g. for Zolpidem, the tolyl and methyl at position 2 and 4 respectively of the imidazo[1,2-*a*]pyridine moiety) and hydroxylation at the heterocycle itself, *ortho* to the methyl substituent (position 7 for Zolpidem), with products that may then be further oxidized and/or conjugated [71]. It also includes hydroxylation of the *N*-alkyl substituents at the amide function (e.g. for Zolpidem and Alpidem, the *N*-methyl and *N*-propyl substituents), ultimately leading to the cleavage of the *N*-alkyl linkage [72]. Metabolites resulting from these biotransformations are more hydrophilic than the parent compound, resulting thus in poor brain penetration of these molecules if any. However, when the phenyl moiety is substituted at the *para* position by an alkoxy group (propoxy or ethoxy in the PET-radiotracers PBR111 and PBR102) [25], additional metabolites resulting from the cleavage of the ether bond have been reported. Besides to the liberation of the corresponding phenolic imidazo[1,2-*a*]pyridine acetamide, small molecules - e.g. fluoropropionate and fluoroacetate

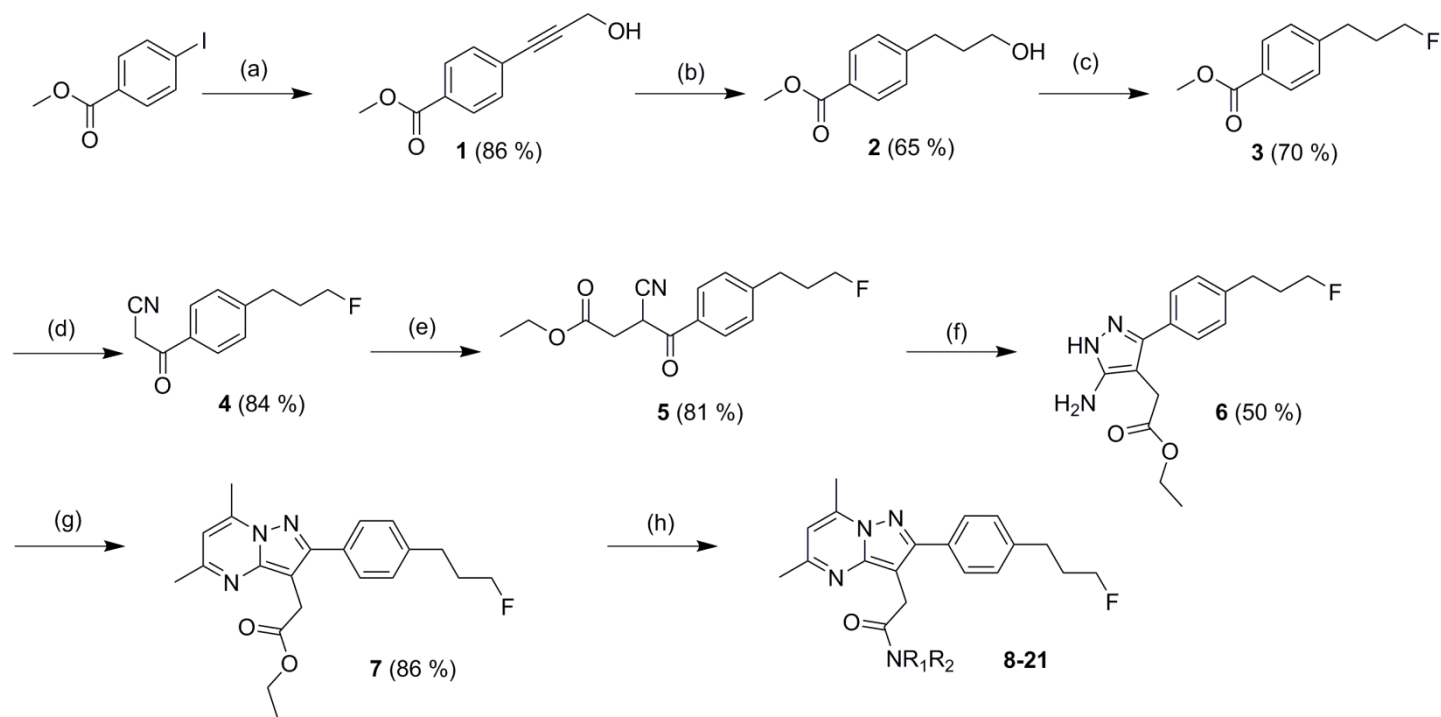
- are produced. The latter are known for penetrating the blood brain barrier (BBB) at various levels, and although lacking any affinity for the target TSPO, accumulate within the brain. When the parent compound is labelled with fluorine-18 (e.g. [¹⁸F]PBR111, [¹⁸F]PBR102), these radiometabolites confound the radioligand concentration measurement and its absolute quantification [73]. Analogous biotransformation pathways have been reported for the pyrazolo[1,5-*a*]pyrimidine acetamide [¹⁸F]DPA-714 [74], where hydroxylations of both methylaryl positions (5 and 7) as well as hydroxylation directly on the pyrazolopyrimidine moiety (position 6, *ortho* to the two previously cited methyl groups) have notably been demonstrated. Cleavage of the fluoroethoxy chain has also been proven, leading to formation and rapid accumulation within the brain of [¹⁸F]fluoroacetate [74].

With the objective of proposing alternative ligands based on the DPA scaffold that would suffer less metabolism particularly regarding the fluoroacetate liberation, we recently synthesized a first series of fluorinated derivatives, in which the oxygen atom bridging the phenyl group and the fluoroalkyl side chain was replaced by, at least, one carbon atom leading to more stable compounds *in vivo* [75]. Among them, the fluoropropyl analogue (CfO-DPA-714) was selected, and labelled with fluorine-18 as a challenger to [¹⁸F]DPA-714 [76]. Herein, we describe the synthesis of a second series of analogues, where the *N,N*-diethylamide part of the structure was pharmaco-modulated, keeping the rest of the scaffold of CfO-DPA-714 unchanged, to investigate the impact of such modifications toward the TSPO affinity and selectivity, lipophilicity for adequate brain entry, and metabolic stability of the molecules. Thus, the replacement of the *N,N*-diethyl substitution at the acetamide part of CfO-DPA-714 was explored with alternative alkyl chains, rigidified motifs, hydrophilic groups or aromatic and more hindered *N*-substituents. For all newly synthesized compounds, TSPO binding affinity and selectivity versus central benzodiazepine receptor (CBR) were evaluated *in vitro*, as well as selected physicochemical parameters such as lipophilicity, topological polar surface area and hydrogen bond donor number. *In vitro* metabolic studies were also conducted using mouse, rat and human microsomes. All data were compared to that of the parent molecules CfO-DPA-714 and DPA-714.

2. Chemistry

Ligands were all developed by modifying the *N,N*-substituents of the acetamide part of CfO-DPA-714. In the pyrazolo[1,2-*a*]pyrimidines series of TSPO ligands, this part of the molecule binds a lipophilic pocket of the protein [13]. Introduction of various alkyl groups to generate asymmetric amides was investigated. Rigidification of the amide substituents was also explored by introducing more or less lipophilic cyclic motifs. Finally, the introduction of more hindered aromatic substituents to the amide nitrogen was also planned as it appears beneficial for the TSPO binding efficiency of other class of ligands featuring acetamides or glyoxylamides moieties [11,13].

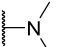
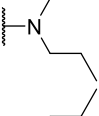
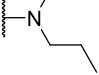
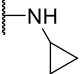
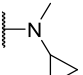
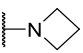
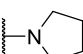
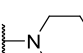
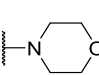
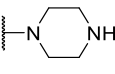
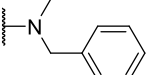
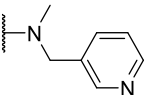
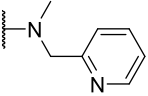
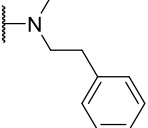
This novel series of pyrazolo[1,5-*a*]pyrimidine acetamides were synthesized in eight chemical steps as depicted in Scheme 1. Note that the synthetic pathway followed for the preparation of this series is quite different from those originally reported for the synthesis of CfO-DPA-714 [75,76], since it is based on the synthesis of a common key ester intermediate (**7**) from which all desired amides could be obtained in one single step.



Scheme 1. Synthesis of new CfO-DPA-714 amide derivatives (**8-21**). **Reagents and conditions:** (a) prop-2-yn-1-ol, CuI, Pd(PPh₃)₂Cl₂, Et₃N, r.t., overnight; (b) H₂, Pd/C 10 %, MeOH, r.t., overnight; (c) Deoxo-Fluor[®] 50 % in THF, DCM, 0 °C to r.t., overnight; (d) i) 2.5 M *n*-BuLi in hexanes, CH₃CN, THF anh., -60 °C, 1 h, then ii) **3**, THF anh., -50 °C to -30 °C, 2 h; (e) NaOH, NaI, BrCH₂CO₂Et, EtOH, r.t., 24 h; (f) NH₂NH₂·H₂O, AcOH, EtOH, reflux, 2 h; (g) acetylacetone, EtOH, reflux, 5 h; (h) i) appropriate amine, AlMe₃, toluene anh., r.t., 1 h, then ii) **7**, toluene anh., heating (70 to 110 °C), 30 min to 5 h.

A Sonogashira coupling reaction of commercially available prop-2-yn-1-ol and methyl 4-iodobenzoate, was first carried out in the presence of Pd(PPh₃)₂Cl₂ and CuI in triethylamine to yield to the propargylic alcohol **1** in 86 % yield. **1** was then treated with hydrogen gas in methanol in the presence of Pd/C for reduction of the triple bond to afford the propanol derivative **2** in 65 % yield. Then, **2** was subjected to a fluorodeoxygenation reaction using Deoxo-Fluor[®] in dichloromethane at room temperature, affording **3** in 70 % yield. The ester function was then converted to the corresponding α -ketonitrile via nucleophilic addition of acetonitrile carbanion, generated with *n*-BuLi as base, at low temperature. These conditions afforded **4** in 84 % yield. Alternatively, the use of sodium methoxide as a base in refluxing acetonitrile was also attempted but proved to be less reproducible with yields ranging from 29 to 76 %. *C*-alkylation using ethyl 2-bromoacetate in the presence of sodium iodide and sodium hydroxide in ethanol at room temperature afforded the ethyl ester **5** in 81 % yield. The latter was then subjected to a first condensation step with hydrazine monohydrate in refluxing acetic acid/ethanol to give the aminopyrazole **6** in 50 % yield. **6** was then subsequently converted into the pyrazolopyrimidine **7** via a second condensation step with acetylacetone in refluxing ethanol (86 % yield). Compound **7**, as a key ester intermediate, was then reacted with various amines, all commercially available with the exception of the *N*-methyl-*N*-cyclopropylamine (**24**) that was prepared as described below (Scheme 2). Reaction was performed in presence of trimethylaluminium in toluene at 110 °C, except for compounds **10** and **16** (100 °C) and compound **13** (70 °C) [77-79]. With the exception of **12**, all the corresponding amides **8-11**, **13-21** were obtained in moderate to good yields (23 to 81 %) and high purities (> 95 %), as summarized in Table 1.

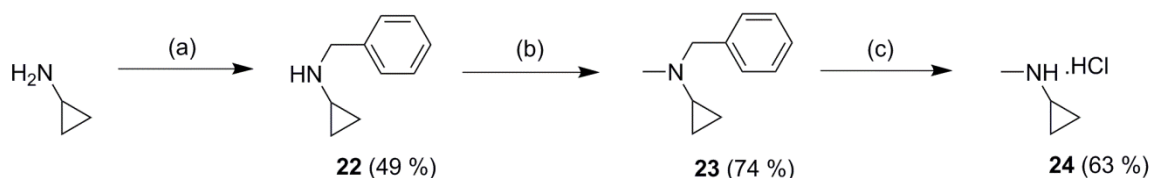
Table 1. CfO-DPA-714 amide analogues (**8-21**) obtained from the common key ester **7**.

Compound	NR ₁ R ₂	Reaction			Purity (HPLC #)
		T (°C)	t (min)	Yield	
8		110	30	66 %	97.1 %
9		110	240	53 %	97.0 %
10		100	60	61 %	95.4 %
11		110	45	81 %	100.0 %
12		110	60	< 5 % *	70.0%
13		70	60	49 %	100.0 %
14		110	60	67 %	100.0 %
15		110	120	61 %	100.0 %
16		100	60	80 %	95.6 %
17		110	60	46 %	98.5 %
18		110	60	62 %	100.0 %
19		110	60	78 %	97.5 %
20		110	300	30 %	96.0 %
21		110	240	23 %	96.4 %

* Conversion rate of **7** to **12** was < 5%, whatever the temperature and reaction time, with notable formation of by-products that did not allow isolation of the desired product with an acceptable purity. # Purity was determined using analytical HPLC (HPLC A, see experimental section).

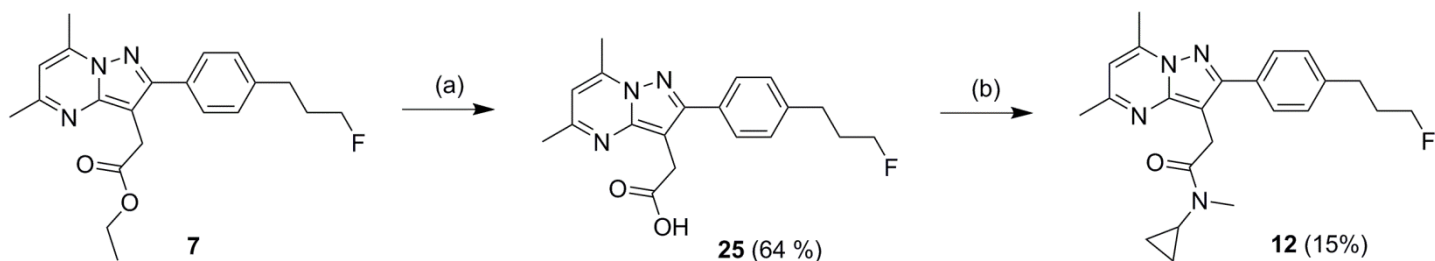
The preparation of the hydrochloride amine salt of *N*-methyl-*N*-cyclopropylamine (**24**) was conducted in three chemical steps according to the procedure described by Yoshida *et al.* [80] (Scheme 2). Briefly, commercially available *N*-cyclopropylamine was protected with a benzyl group using benzyl bromide and triethylamine in THF at room temperature to afford the *N*-benzyl-*N*-cyclopropylamine **22** with 49 % yield. Compound **22** was subsequently *N*-methylated by reductive amination in presence of

paraformaldehyde and sodium borohydride at 0 °C to give **23** in 74 % yield. Cleavage of the benzyl group (performed using hydrogen gas in methanol in presence of 10 % Pd/C) followed by treatment with an excess of a 10 M methanolic solution of hydrochloric acid afforded the desired hydrochloride salt **24** with 63 % yield.



Scheme 2. Synthesis of *N*-methyl-*N*-cyclopropylamine hydrochloride **24**. **Reagents and conditions:** (a) BnBr, Et₃N, THF, r.t., overnight; (b), 37 % wt. CH₂O, NaBH₄, 0 °C, 30 min; (c) i) H₂, Pd/C 10 %, MeOH, r.t., overnight, ii) 10 M HCl in MeOH.

Finally, the preparation of the *N*-methyl-*N*-cyclopropylamide derivative **12**, which is a disubstituted amide with expected steric and lipophilic properties in between the cycloalkyl-substituted amides **13** (azetidine) or **14** (pyrrolidine) and the dialkyl compounds **8** (*N,N*-dimethyl), **9** (*N*-methyl-*N*-propyl) or CfO-DPA-714 (*N,N*-diethyl), was also attempted following two alternative pathways. The first one was a direct *N*-methylation of its analogue **11**, using sodium hydride and iodomethane in DMF at room temperature. However, due to the poor selectivity of these reaction conditions, the formation of several by-products was observed, preventing isolation of **12** in acceptable amount and purity. The second one was a peptide-like coupling reaction involving the previously described amine **24**, and the carboxylic acid **25** resulting from hydrolysis of ester **7** as depicted in scheme 3.



Scheme 3. Synthesis of the *N*-methyl-*N*-cyclopropylamide derivative **12**. **Reagents and conditions:** (a) KOH, MeOH, 40 °C, 3 h; (b) **24**, Et₃N, TBTU, DCM, r.t., 12 h.

Thus, **7** was hydrolysed using potassium hydroxide in methanol at 40 °C to give **25** in 64 % yield, that was subsequently coupled with amine **24** in presence of TBTU as catalyst agent and triethylamine as base, in dichloromethane at room temperature. Using these conditions, the *N*-methyl-*N*-cyclopropylamide **12** could be synthesized in up to 15 % yield, but with a maximum purity of 70 % (based on HPLC analyses). None of the alternative synthetic pathways led to satisfactory production of **12** and determination of its binding affinity for the TSPO was not considered then.

3. Results and discussion

The binding affinity for the TSPO of all newly synthesized derivatives were measured by competition experiments against [³H]PK11195 in membrane homogenates of rat heart. Binding affinities were also evaluated for the CBR by competitive assays against [³H]flunitrazepam using membrane homogenates of rat cerebral cortex. The inhibition constant (TSPO K_i) and percentage of inhibition at 1 μM (CBR), determined for each compound, are reported in Table 2. The lipophilicity parameter logD_{7.4} was also

evaluated for each new compound of this series, based on their HPLC retention time. Additionally, cLogP, topological polar surface area (TPSA), number of hydrogen bond donors (HBD) and molecular size (as molecular weight (MW)) were also calculated for all derivatives. Data, including those belonging to the lead compound DPA-714 and its analogue (CfO-DPA-714) for comparison, are summarized in Table 2.

Table 2. *In vitro* competitive binding assays, lipophilicity, topological polar surface area, HBD and MW of DPA-714, CfO-DPA-714 and the fluorinated analogues **8-11**, **13-21**.

Ligand	TSPO ^a K _i (nM)	CBR % inhib. ^b at 1 μM	LogD _{7.4} ^c	clogP ^d	TPSA ^d (Å ²)	HBD	MW
DPA-714	0.91 ± 0.08	0 %	2.89	3.33	57.5	0	398
CfO-DPA-714	0.37 ± 0.02	0 %	3.51	3.99	48.3	0	396
8	15 ± 1	2 %	2.68	2.93	48.3	0	368
9	0.25 ± 0.01	0 %	3.65	3.99	48.3	0	396
10	0.26 ± 0.01	0 %	4.39	4.99	48.3	0	424
11	17 ± 2	0 %	2.69	3.23	57.1	1	380
13	32 ± 2	0 %	2.73	3.10	48.3	0	380
14	26 ± 3	0 %	3.04	3.65	48.3	0	394
15	2.2 ± 0.3	0 %	3.56	4.21	48.3	0	408
16	27 ± 1	0 %	2.56	3.21	57.5	0	410
17	260 ± 11	0 %	0.87	3.20	60.3	1	409
18	0.30 ± 0.02	0 %	3.98	4.62	48.3	0	444
19	2.8 ± 0.1	0 %	2.61	3.12	60.6	0	445
20	1.2 ± 0.1	0 %	3.16	3.12	60.6	0	445
21	1.1 ± 0.2	0 %	4.08	5.03	48.3	0	458

^a TSPO K_i values (mean ± SD, duplicate) were determined using membrane homogenates of rat heart and screened against [³H]PK11195 (K_d = 1.8 nM, c = 0.2 nM).

^b CBR binding affinity was evaluated using homogenates of rat cerebral cortex and expressed as % of inhibition at 1 μM against [³H]flunitrazepam (K_d = 2.1 nM, c = 0.4 nM).

^c LogD_{7.4} were determined by converting the retention time recorded for the tested compounds using a validated, standardized HPLC method.

^d cLogP and TPSA were both determined using ChemDraw 15.0 software.

As shown in Table 2, and with the exception of the piperazinamide **17** (260 nM), all synthesized compounds displayed nanomolar to subnanomolar binding affinity for the TSPO, with K_i values ranging from 0.25 nM to 32 nM. Within this series, the *N*-methyl-*N*-phenethylamide **21** and both *N*-methyl-*N*-pyridinylmethylamides **19** and **20** showed values (1.1, 2.8 and 1.2 nM respectively) comparable to that of DPA-714 (0.91 nM). Three compounds - i.e. the *N*-methyl-*N*-propylamide **9**, the *N,N*-dipropylamide **10** and the *N*-methyl-*N*-benzylamide **18** - displayed subnanomolar affinities with K_i values even slightly lower to that of CfO-DPA-714 (0.37 nM): 0.25, 0.26 and 0.30 nM respectively. It can be seen that shortening of the *N,N*-alkyl substituents (compound **8**) or rigidification of the groups at the amide nitrogen are not beneficial to TSPO binding (compounds **11**, **13**, **14**, **16** and **17**) especially when the substituent features an heteroatom (compounds **16** and **17**). Interestingly, the introduction of a bulky aromatic substituent (compounds **18-21**) does not dramatically affect the TSPO binding efficiency and seems to be rather favourable in the case of compound **18**. As a general trend, the more lipophilic the *N*-substituents are, the best the TSPO binding affinity of the corresponding molecule is: i) compounds with logD_{7.4} values above 3.1 exhibited the lowest TSPO K_i constants (see compounds **9**, **10**, **15**, **18**, **20** and **21**); ii) the introduction of a heteroatom on the benzyl moiety - leading to an increase of the hydrophilic character of the structure - led to a decrease of the TSPO binding affinity: compare **19** and **20** to **18**. Interestingly, the replacement of an *N*-benzyl with an *N*-phenethyl substituent (compare compounds **18** and **21**) led to a one log decrease of affinity, probably due to an unfavourable steric interaction

with a lipophilic binding pocket of the protein [81]. All compounds showed no (or negligible, i.e. 2% for the *N,N*-dimethylamide **8**) inhibition of [³H]flunitrazepam binding to the CBR at 1 μ M, attesting the excellent selectivity toward the TSPO.

These findings are also in accordance with previous quantitative structure-activity relationship (QSAR) studies performed on imidazo[1,2-*a*]pyridine acetamides [82-84], for which in terms of both the affinity to the TSPO (previously named PBR for peripheral benzodiazepine receptor) and the selectivity toward the CBR, i) a di-substituted amide pattern was preferred to a single substitution of the nitrogen; ii) an optimal combination and the length of the linear or conformationally restricted alkyl substituents is of fundamental importance; iii) the presence of an aromatic moiety may be advantageous due to a potential hydrophobic π - π interaction with a tryptophan residue in the binding pocket and iv) a substitution at the *para* position of the phenyl moiety carried by the heterocycle is well tolerated and even beneficial.

Lipophilicity, TPSA, number of HBD and molecular size (MW) are the admitted four key-parameters influencing passive BBB diffusion. As such, compounds targeting the CNS are usually associated with lipophilicity values (cLogP, LogD) in the range of 2 to 5, small TPSAs (< 90 \AA^2 , even preferably < 70 \AA^2), absence (or not more than one) HBD and a MW below 500 Da [85]. As shown in Table 2, all synthesized compounds showed calculated LogP and measured LogD_{7.4} values below 5. Good correlation between these values was found, with LogD_{7.4} generally 15 to 25 % lower than the corresponding cLogP with one exception, the piperazinamide **17**. Among the compounds displaying good binding affinity for the TSPO (K_i < 3.0 nM), **9** and **15** exhibited very similar logD_{7.4} values to CfO-DPA-714 (3.64 and 3.56 versus 3.51). Compounds **19** and **20** are less lipophilic molecules, due to the presence of an heteroatom at the *N*-substituted position of the amide, with logD_{7.4} values in the range of that of DPA-714 (2.61 and 3.16 versus 2.89), while compounds **10**, **18** and **21** are more lipophilic structures with logD_{7.4} greater than that of CfO-DPA-714 (4.39, 3.98 and 4.08 respectively). TPSA values are also all well below the given cut-off values for optimal brain penetration (48.3 \AA^2 to 60.6 \AA^2). Moreover, MW of all synthesized compounds range between 369 and 459 g/mol. Absence of HBD is also demonstrated for almost all compounds, only the *N*-cyclopropylamine **11** and the piperazinamide **17** showing a HBD number of 1.

Table 3. *In vitro* microsomal stability of DPA-714, CfO-DPA-714 and compounds **9**, **10**, **15**, **18-21**.

Compound	Intrinsic clearance (InC, μ L/min/mg protein) ^a		
	Human	Rat	Mouse
DPA-714	68	> 1000	408
CfO-DPA-714	241	>1000	865
9	321	> 1000	781
10	> 1000	> 1000	> 1000
15	424	> 1000	931
18	> 1000	> 1000	> 1000
19	862	> 1000	> 1000
20	270	610	947
21	> 1000	> 1000	> 1000

^aintrinsic clearance, expressed as μ L/min/mg protein, reflects the rate of biotransformation of a compound. Its calculation is detailed in the experimental section.

The synthesized analogues with TSPO K_i values below 3.0 nM (e.g. **9**, **10**, **15**, **18-21**) were evaluated for their *in vitro* microsomal metabolic stability using three different species: human, rat and mouse, as presented in Table 3. The results, expressed as the intrinsic clearance (InC, μ L/min/mg protein, see experimental section for calculation), reflect the *in vivo* metabolic biotransformation of the

compounds: the more the value is elevated, the more the compound is metabolized. DPA-714 and CfO-DPA-714 were also tested as references. As shown in Table 3, all compounds (including DPA-714 and CfO-DPA-714) were rapidly metabolized in presence of rat microsomes, with InC values above 1000, excepted for compound **20** that seemed slightly more stable (610 $\mu\text{L}/\text{min}/\text{mg}$ protein). All newly synthesized compounds, as well as CfO-DPA-714, were also rapidly biotransformed in the presence of mouse microsomes (InC values above 750 $\mu\text{L}/\text{min}/\text{mg}$ protein). However, in the presence of human microsomes, biotransformation rates were more variable, with InC values ranging from 270 (compound **20**) to more than 1000 $\mu\text{L}/\text{min}/\text{mg}$ protein (compounds, **10**, **18** and **21**). Compounds **9** and **20** stand out as the less metabolized ones with InC values of 321 and 270 $\mu\text{L}/\text{min}/\text{mg}$ protein, respectively. This rate of metabolization is in the range of what has been observed with CfO-DPA-714 (241 $\mu\text{L}/\text{min}/\text{mg}$ protein). Interestingly, DPA-714 remained the most stable compound in both mouse and human microsomal incubations.

4. Conclusion

A novel series of analogues of CfO-DPA-714, modified at the amide part, were synthesized and *in vitro* evaluated for their potential to bind the TSPO. Their TSPO/CBR binding selectivity, their lipophilicity ($\text{LogD}_{7.4}$) and a few selected physicochemical parameters (cLogP, TPSA and HBD number), as well as their stability in the presence of mouse, rat and human microsomes were also assessed. Among these new analogues, compounds **9**, **10** and **18** (TSPO K_i : 0.25, 0.26 and 0.30 nM respectively) stand out as promising candidates for drug development, with a preference for compound **9** based on its *in vitro* metabolic stability. The present work, without claiming to solve all metabolic issues related to the pyrazolo[1,5-*a*]pyrimidine scaffold, confirms the interest of the carbon-for-oxygen substitution in the fluorine-bearing moiety already demonstrated for CfO-DPA-714, and provides novel opportunities for fluorine-18-labelling as well as for the development of *in vivo* PET-probes for neuroinflammation imaging.

5. Experimental section

5.1. Chemistry

General. Chemicals were purchased from Aldrich France and were used without further purification. Flash chromatographies were conducted on silica gel (0.63-0.200 mm, VWR France) columns. TLCs were run on aluminium pre-coated plates of silica gel 60F₂₅₄ (VWR France). The compounds were localized at 254 nm using a UV-lamp and by dipping the TLC-plates in a basic potassium permanganate aqueous solution and heating on a hot plate. ¹H and ¹³C NMR spectra were recorded on a Bruker (Wissembourg, France) Avance 400 MHz apparatus and chemical shifts were referenced to the hydrogenated residue of the deuterated solvent ($\delta[\text{CHCl}_3] = 7.23$ ppm and $\delta[\text{CD}_2\text{HOD}] = 3.31$ ppm) for ¹H NMR and to the deuterated solvent ($\delta[\text{CDCl}_3] = 77.0$ ppm and $\delta[\text{CD}_3\text{OD}] = 49.2$ ppm) for ¹³C NMR experiments. The typical standard concentration of the analysed samples was 20 mg/mL. The chemical shifts are reported in ppm, downfield from TMS (s, d, t, q, q⁵, sex, m and b for singlet, doublet, triplet, quadruplet, quintuplet, sextuplet, multiplet and broad, respectively). High resolution mass spectrometry (HRMS) determination has benefited from the facilities and expertise of scientific service, HPLC-Mass spectrometry of ICSN, CNRS, Gif sur Yvette, France (www.icsn.cnrs-gif.fr); analyses were performed by electrospray with positive (ESI+) or negative (ESI-) ionization mode. Purity of the synthesized compounds was determined using analytical HPLC (HPLC A): UPLC/SQD Acquity Waters, Acquity BEH C18 (2.1 x 50 mm, 1.7 μm) column, mobile phase: H₂O (A), CH₃CN + 0.1 % formic acid (B), gradient: 2 to 100 % (B) in 3 min, 1.0 mL/min, and was found to be greater than 95% in all cases. $\text{LogD}_{7.4}$ values were determined based on a validated and standardized HPLC method (HPLC B): Alliance 2695 - PDA Waters, X-Terra MS C18 (4.6 x 20 mm, 3.5 μm) column, mobile phase: 5 mM MOPS/(CH₃)₄NOH pH 7.4 (A), 5 % MOPS/(CH₃)₄NOH (100 mM, pH 7.4) / 95 % CH₃CN (B), gradient (A/B): 98:2 (0.5 min), 0:100 (4.8 min), 98:2 (1.6 min), 1.2 mL/min, 25 °C, detection at 254 nm.

Methyl 4-(3-hydroxyprop-1-yn-1-yl)benzoate (1). To a solution of methyl 4-iodobenzoate (25 g, 95.4 mmol) in triethylamine (500 mL) was added prop-2-yn-1-ol (6.7 mL, 115 mmol, 1.2 eq.). The reaction mixture was degassed under vacuum and filled with argon (2 cycles). Then, palladium bis(triphenylphosphine)dichloride (670 mg, 0.95 mmol, 1 mol %) and copper iodide (182 mg, 0.95 mmol, 1 mol %) were added to the suspension and the reaction mixture was stirred at room temperature overnight. Then, it was concentrated to dryness and the residue was dissolved in ethyl acetate (400 mL). The resulting solution was washed successively with a 1.0 M aqueous hydrochloric acid solution (100 mL), water (2 x 200 mL), brine (200 mL), then dried over sodium sulfate, filtered and concentrated to dryness. The residue was purified by flash chromatography on silica gel (heptane/ethyl acetate 60/40) to afford **1** (15.6 g, 86 %) as a yellow crystalline powder. R_f (heptane/ethyl acetate 60/40): 0.24. Mp: 85-86 °C. $^1\text{H NMR}$ (CDCl_3) δ 7.98 (d, $J = 8.0$ Hz, 2H), 7.48 (d, $J = 8.0$ Hz, 2H), 4.52 (d, $J = 4.4$ Hz, 2H), 3.90 (s, 3H), 1.93 (bt, $w_{1/2} = 13$ Hz, 1H, OH). $^{13}\text{C NMR}$ (CDCl_3) δ 166.5 [C], 131.5 [2xCH], 129.7 [C], 129.4 [2xCH], 127.2 [C], 90.1 [C], 84.8 [C], 52.2 [CH₃], 51.5 [CH₂].

Methyl 4-(3-hydroxypropyl)benzoate (2). To a solution of **1** (10.0 g, 52.6 mmol) in methanol (250 mL) was cautiously added 10 % palladium on charcoal in one portion to each reaction mixture (400 mg, 3.7 mmol, 40 mg/g). Then, each reaction flask was degassed and filled with hydrogen at 1 atm. The reaction mixture was stirred at ambient temperature overnight and the balloon was refilled when necessary. Once completed (NMR monitoring), the reaction mixture was cautiously filtered on a pad of Celite[®] and the catalyst was washed with dichloromethane/methanol 80/20 (500 mL). The filtrate was concentrated to dryness and the residue was purified by flash chromatography on silica gel (heptane/ethyl acetate 50/50) to afford **2** (6.7 g, 65 %) as an orange oil. R_f (heptane/ethyl acetate 50/50): 0.18. $^1\text{H NMR}$ (CDCl_3) δ 7.93 (d, $J = 8.0$ Hz, 2H), 7.24 (d, $J = 8.0$ Hz, 2H), 3.88 (s, 3H), 3.65 (t, $J = 6.4$ Hz, 2H), 2.74 (t, $J = 7.6$ Hz, 2H), 2.36 (s, 1H), 1.88 (tt, $J = 7.6$ & 6.4 Hz, 2H). $^{13}\text{C NMR}$ (CDCl_3) δ 167.2 [C], 147.5 [C], 129.6 [2xCH], 128.4 [2xCH], 127.6 [C], 61.7 [CH₂], 51.9 [CH₃], 33.7 [CH₂], 32.0 [CH₂].

Methyl 4-(3-fluoropropyl)benzoate (3). To a solution of **2** (5.00 g, 25.7 mmol) in dichloromethane (200 mL) cooled at 0 °C was added dropwise a 50 % Deoxo-Fluor[®] solution in THF (20 mL, excess) over 15 min. The reaction mixture was warmed up to ambient temperature and stirred overnight. Then, it was cooled at 0 °C and water (100 mL) was slowly and cautiously added. The organic layer was separated, washed with water (2 x 100 mL) and brine (100 mL), dried over sodium sulfate, filtered and concentrated to dryness. The residue was purified by flash chromatography on silica gel (heptane/ethyl acetate 90/10 to 50/50) to afford **3** (3.55 g, 70%) as a yellow oil. R_f (heptane/ethyl acetate 50/50): 0.52. $^1\text{H NMR}$ (CDCl_3) δ 7.96 (d, $J = 8.0$ Hz, 2H), 7.26 (d, $J = 8.0$ Hz, 2H), 4.44 (dt, $J_{\text{HF}}^2 = 47.2$ Hz, $J_{\text{HH}}^3 = 6.0$ Hz, 2H), 3.89 (s, 3H), 2.80 (t, $J = 7.6$ Hz, 2H), 2.01 (dtt, $J_{\text{HF}}^3 = 27.2$ Hz, $J_{\text{HH}}^3 = 7.6$ & 6.0 Hz, 2H). $^{13}\text{C NMR}$ (CDCl_3) δ 166.9 [C], 146.5 [C], 129.7 [2xCH], 128.4 [2xCH], 128.0 [C], 82.8 [d, $J_{\text{CF}}^1 = 164$ Hz, CH₂], 51.9 [CH₃], 31.6 [d, $J_{\text{CF}}^2 = 19$ Hz, CH₂], 31.3 [d, $J_{\text{CF}}^3 = 5$ Hz, CH₂].

3-(4-(3-Fluoropropyl)phenyl)-3-oxopropanenitrile (4). To anhydrous tetrahydrofuran (50 mL) cooled at -60 °C, was carefully added a 2.5 M *n*-butyllithium solution in hexanes (23 mL, 57.5 mmol). A solution of acetonitrile (3.0 mL, 57.8 mmol) in anhydrous tetrahydrofuran (10 mL) was cautiously added dropwise while maintaining the temperature below -50 °C. The reaction mixture was stirred for 1 h at -60 °C. Then, a solution of **3** (3.78 g, 19.3 mmol) in anhydrous tetrahydrofuran (50 mL) was gently added to the mixture over 15 min while maintaining the temperature below -50 °C. After the addition, the content was stirred for an additional 2 h at -50 °C and the reaction was then quenched with methanol (10 mL) at -40 °C, poured into water (400 mL) and acidified with a 37 % aqueous hydrochloric acid solution to pH 3. The mixture was extracted with ethyl acetate (2 x 200 mL) and the combined organic layers were then washed with water (2 x 100 mL) and brine (100 mL), dried over sodium sulfate, filtered and concentrated to dryness. The residue was purified by flash chromatography on silica gel (heptane/ethyl acetate 70/30 to 60/40) to afford **4** (3.33 g, 16.2 mmol) as white crystals (84 %). R_f (heptane/ethyl acetate 50/50): 0.37. Mp: 63-64 °C. $^1\text{H NMR}$ (CDCl_3) δ 7.86 (d, $J = 8.0$ Hz, 2H), 7.35 (d, J

= 8.0 Hz, 2H), 4.46 (dt, $J_{\text{HF}}^2 = 47.2$ Hz, $J_{\text{HH}}^3 = 6.0$ Hz, 2H), 4.07 (s, 2H), 2.84 (t, $J = 7.6$ Hz, 2H), 2.04 (dt, $J_{\text{HF}}^3 = 25.6$ Hz, $J_{\text{HH}}^3 = 7.6$ & 6.0 Hz, 2H). ^{13}C NMR (CDCl_3) δ 186.6 [C], 148.9 [C], 132.3 [C], 129.2 [2xCH], 128.7 [2xCH], 113.8 [C], 82.7 [d, $J_{\text{CF}}^1 = 164$ Hz, CH_2], 31.5 [d, $J_{\text{CF}}^3 = 5$ Hz, CH_2], 31.4 [d, $J_{\text{CF}}^2 = 20$ Hz, CH_2], 29.3 [CH_2].

Ethyl 3-cyano-4-(4-(3-fluoropropyl)phenyl)-4-oxobutanoate (5). To a solution of **4** (5.34 g, 26.0 mmol) in ethanol (150 mL) was added in one portion, under vigorous stirring, sodium hydroxide (1.14 g, 28.6 mmol). The reaction mixture was stirred at ambient temperature for 15 min. Then, sodium iodide (3.90 g, 26.0 mmol) and ethyl bromoacetate (3.18 mL, 28.6 mmol) were added to the reaction mixture which was stirred at ambient temperature for 24 h. The reaction mixture was concentrated to dryness and the residue was partitioned between acidified water (100 mL, pH 1) and ethyl acetate (200 mL). The organic layer was separated, washed with water (200 mL) and brine (100 mL), dried over sodium sulfate, filtered and concentrated to dryness. The residue was purified by flash chromatography on silica gel (heptane/ethyl acetate 80/20 to 50/50) to afford **5** (6.15 g, 81%) as a yellow oil. R_f (heptane/ethyl acetate 50/50): 0.5. ^1H NMR (CDCl_3) δ 7.98 (d, $J = 8.0$ Hz, 2H), 7.36 (d, $J = 8.0$ Hz, 2H), 4.74 (dd, $J = 8.4$ & 5.6 Hz, 1H), 4.46 (dt, $J_{\text{HF}}^2 = 47.2$ Hz, $J_{\text{HH}}^3 = 5.6$ Hz, 2H), 4.18 (q, $J = 7.6$ Hz, 2H), 3.26 (dd, $J = 17.2$ & 8.4 Hz, 1H), 2.92 (dd, $J = 17.2$ & 5.6 Hz, 1H), 2.84 (t, $J = 7.6$ Hz, 2H), 2.04 (dt, $J_{\text{HF}}^3 = 19.6$ Hz, $J_{\text{HH}}^3 = 7.6$ & 5.6 Hz, 2H), 1.26 (t, $J = 7.2$ Hz, 3H). ^{13}C NMR (CDCl_3) δ 188.0 [C], 169.5 [C], 148.9 [C], 131.8 [C], 129.3 [2xCH], 129.2 [2xCH], 116.4 [C], 82.6 [d, $J_{\text{CF}}^1 = 165$ Hz, CH_2], 61.6 [CH_2], 34.1 [CH], 32.8 [CH_2], 31.5 [d, $J_{\text{CF}}^3 = 5$ Hz, CH_2], 31.4 [d, $J_{\text{CF}}^2 = 20$ Hz, CH_2], 14.0 [CH_3].

Ethyl 2-(5-amino-3-(4-(3-fluoropropyl)phenyl)-1H-pyrazol-4-yl)acetate (6). To a solution of **5** (6.15 g, 21.1 mmol) in ethanol (120 mL) were added dropwise, at ambient temperature, monohydrated hydrazine (3 mL, 63.3 mmol) and acetic acid (2 mL, 35.8 mmol). The reaction mixture was refluxed for 2 h. Then, it was concentrated to dryness and the residue was partitioned between ethyl acetate (50 mL) and a 10 % potassium carbonate aqueous solution (20 mL). The organic layer was separated, washed with water (2 x 20 mL) and brine (20 mL), dried over sodium sulfate, filtered and concentrated to dryness. The residue was purified by flash chromatography on silica gel (dichloromethane/methanol 97/3) to afford **6** (3.25g, 50 %) as an orange oil. R_f (dichloromethane/methanol 95/5): 0.38. ^1H NMR (CDCl_3) δ 7.45 (d, $J = 8.0$ Hz, 2H), 7.26 (d, $J = 8.0$ Hz, 2H), 6.24 (b, $w_{1/2} = 88$ Hz, 3H), 4.46 (dt, $J_{\text{HF}}^2 = 47.2$ Hz, $J_{\text{HH}}^3 = 6.0$ Hz, 2H), 4.17 (q, $J = 7.2$ Hz, 2H), 3.41 (s, 2H), 2.77 (t, $J = 7.6$ Hz, 2H), 2.08-1.95 (m, 2H), 1.27 (t, $J = 7.2$ Hz, 3H). ^{13}C NMR (CDCl_3) δ 171.9 [C], 153.8 [C], 143.0 [C], 141.7 [C], 129.0 [2xCH], 127.8 [2xCH], 127.7 [C], 96.8 [C], 82.9 [d, $J_{\text{CF}}^1 = 164$ Hz, CH_2], 61.1 [CH_2], 31.8 [d, $J_{\text{CF}}^2 = 19$ Hz, CH_2], 31.0 [d, $J_{\text{CF}}^3 = 5$ Hz, CH_2], 29.4 [CH_2], 14.1 [CH_3].

Ethyl 2-(2-(4-(3-fluoropropyl)phenyl)-5,7-dimethylpyrazolo[1,5-a]pyrimidin-3-yl)acetate (7). To a solution of **6** (748 mg, 2.44 mmol) in ethanol (50 mL) was added acetylacetone (0.50 mL, 4.87 mmol). The reaction mixture was refluxed for 5 h. Once the reaction completed, the mixture was concentrated to dryness and the residue was dissolved in ethyl acetate (100 mL). The solution was then washed with water (2 x 50 mL) and brine (50 mL), dried over sodium sulfate, filtered and concentrated to dryness. The residue was purified by flash chromatography on silica gel (dichloromethane/methanol 99/1 to 98/2) to afford **7** (773 mg, 86 %) as light yellow crystals. R_f (dichloromethane/methanol 96/4): 0.60. ^1H NMR (CDCl_3) δ 7.70 (d, $J = 8.0$ Hz, 2H), 7.30 (d, $J = 8.0$ Hz, 2H), 6.54 (s, 1H), 4.47 (dt, $J_{\text{HF}}^2 = 47.2$ Hz, $J_{\text{HH}}^3 = 6.0$ Hz, 2H), 4.13 (q, $J = 7.2$ Hz, 2H), 3.97 (s, 2H), 2.80 (t, $J = 7.6$ Hz, 2H), 2.75 (s, 3H), 2.57 (s, 3H), 2.04 (dt, $J_{\text{HF}}^3 = 26.8$ Hz, $J_{\text{HH}}^3 = 7.6$ & 6.0 Hz, 2H), 1.19 (t, $J = 7.2$ Hz, 3H). ^{13}C NMR (CDCl_3) δ 171.8 [C], 157.9 [C], 154.7 [C], 147.6 [C], 144.8 [C], 141.4 [C], 131.3 [C], 128.7 [2xCH], 128.4 [2xCH], 108.5 [CH], 99.4 [C], 83.0 [d, $J_{\text{CF}}^1 = 164$ Hz, CH_2], 60.7 [CH_2], 31.9 [d, $J_{\text{CF}}^2 = 20$ Hz, CH_2], 31.0 [d, $J_{\text{CF}}^3 = 5$ Hz, CH_2], 29.2 [CH_2], 24.6 [CH_3], 16.8 [CH_3], 14.1 [CH_3].

General procedure for the preparation of compounds 8-21: To a solution of the appropriate amine (4 eq) in anhydrous toluene (3 mL) was added dropwise, under argon and at room temperature, a 2.0 M trimethylaluminium solution in toluene (3 to 4 eq). The

resulting solution was stirred at room temperature for 1 h. Then, a solution of the ester **7** (50-300 mg, 1 eq) in toluene (1 mL) was added in one portion and the mixture was heated at 110 °C (except otherwise stated) until completion (TLC) of the reaction. The mixture was then quenched with water (20 mL) and further diluted with a 0.1 M hydrochloric acid aqueous solution (10 mL), unless otherwise stated. The mixture was finally extracted twice with ethyl acetate (2 x 20 mL) and the combined organic layers were washed with water (20 mL) and brine (10 mL), dried over sodium sulfate, filtered and concentrated to dryness. The residue was either triturated in diethyl ether (2 mL) or purified by flash chromatography on silica gel (using dichloromethane/methanol 99/1 to 94/6 or dichloromethane/acetone 95/5 to 85/15) to afford the desired products **8** to **21**.

2-(2-(4-(3-Fluoropropyl)phenyl)-5,7-dimethylpyrazolo[1,5-a]pyrimidin-3-yl)-N,N-dimethylacetamide (8). This amide was prepared following the general procedure described above using 50 mg of the ester **7** (0.135 mmol), 44 mg of *N,N*-dimethylamine hydrochloride (4 eq, 0.540 mmol), 271 μ L of 2.0 M trimethylaluminium solution in toluene (4 eq, 0.542 mmol), and heating for 30 min. **8** (30 mg, 60 %) was obtained as beige crystals after trituration in diethyl ether. R_f (dichloromethane/methanol 97/3): 0.20. t_R (HPLC A) = 1.18 min (purity: 97.1 %). Mp: 162-164 °C. ^1H NMR (CDCl_3) δ 7.75 (d, $J = 8.0$ Hz, 2H), 7.29 (d, $J = 8.0$ Hz, 2H), 6.52 (s, 1H), 4.48 (dt, $J_{\text{HF}}^2 = 47.2$ Hz, $J_{\text{HH}}^3 = 6.0$ Hz, 2H), 3.94 (s, 2H), 3.16 (s, 3H), 2.98 (s, 3H), 2.79 (t, $J = 7.6$ Hz, 2H), 2.75 (s, 3H), 2.55 (s, 3H), 2.04 (dq 5 , $J_{\text{HF}}^3 = 25.2$ Hz, $J_{\text{HH}}^3 = 7.6$ Hz, 2H). ^{13}C NMR (CDCl_3) δ 170.8 [C], 157.5 [C], 155.1 [C], 147.4 [C], 144.9 [C], 141.2 [C], 131.5 [C], 128.7 [2xCH], 128.7 [2xCH], 108.3 [CH], 100.6 [C], 83.0 [d, $J_{\text{CF}}^1 = 163$ Hz, CH_2], 37.6 [CH_3], 35.8 [CH_3], 31.9 [d, $J_{\text{CF}}^2 = 20$ Hz, CH_2], 31.1 [d, $J_{\text{CF}}^3 = 5$ Hz, CH_2], 28.2 [CH_2], 24.6 [CH_3], 16.9 [CH_3]. HR-ESI(+)-MS m/z calcd for $\text{C}_{21}\text{H}_{25}\text{FN}_4\text{O}$: 369.2085 [$\text{M}+\text{H}$] $^+$, found 369.2087.

2-(2-(4-(3-Fluoropropyl)phenyl)-5,7-dimethylpyrazolo[1,5-a]pyrimidin-3-yl)-N-methyl-N-propylacetamide (9). This amide was prepared following to the general procedure described above using 300 mg of the ester **7** (0.81 mmol), 118 mg of *N*-methyl-*N*-propylamine (2 eq, 1.62 mmol), 163 μ L of 2 M trimethylaluminium solution in toluene (4 eq, 3.24 mmol), and heating for 4 h. **9** was obtained as light yellow solid after flash chromatography on silica gel (dichloromethane/acetone 95/5 to 85/15) (170 mg, 53 %). R_f (dichloromethane/acetone 90/10): 0.22. t_R (HPLC A) = 1.39 min (purity: 97.0 %). Mp: 122-124 °C. ^1H NMR (CDCl_3 , 400 MHz) δ 7.75 (d, 2H, $J = 8.0$ Hz), 7.28 (d, 2H, $J = 8.0$ Hz), 6.51 (s, 1H), 4.52 (dt, 2H, $J_{\text{HF}}^2 = 47.2$ Hz, $J_{\text{HH}}^3 = 6.0$ Hz), 3.94 (s, 1H, *rot A*), 3.92 (s, 1H, *rot B*), 3.42 (t, 1H, $J = 7.2$ Hz, *rot A*), 3.36 (t, 1H, $J = 7.2$ Hz, *rot B*), 3.12 (s, 1.5H, *rot A*), 2.95 (s, 1.5H, *rot B*), 2.79 (t, 2H, $J = 7.2$ Hz), 2.74 (s, 3H), 2.54 (s, 3H), 2.03 (dq 5 , 2H, $J_{\text{HF}}^3 = 25.2$ Hz, $J_{\text{HH}}^3 = 7.2$ Hz), 1.65 (q 5 , 1H, $J = 7.2$ Hz, *rot A*), 1.54 (q 5 , 1H, $J = 7.2$ Hz, *rot B*), 0.91 (t, 1.5H, $J = 7.2$ Hz, *rot A*), 0.87 (t, 1.5H, $J = 7.2$ Hz, *rot B*). ^{13}C NMR (CDCl_3 , 100 MHz) δ 170.6 [C, *rot A*], 170.5 [C, *rot B*], 157.4 [C], 155.0 [C], 174.5 [C], 144.4 [C], 141.1 [C], 131.5 [C], 128.7 [2xCH], 128.6 [2xCH], 108.2 [CH], 100.8 [C], 82.9 [d, $J_{\text{CF}}^1 = 164$ Hz, CH_2], 51.6 [CH_2 , *rot A*], 49.6 [CH_2 , *rot B*], 35.6 [CH_3 , *rot A*], 33.7 [CH_3 , *rot B*], 31.9 [d, $J_{\text{CF}}^2 = 19$ Hz, CH_2], 31.0 [d, $J_{\text{CF}}^3 = 5$ Hz, CH_2], 28.4 [CH_2 , *rot A*], 27.9 [CH_2 , *rot B*], 24.5 [CH_3], 21.5 [CH_2 , *rot A*], 20.3 [CH_2 , *rot B*], 16.8 [CH_3], 11.1 [CH_3 , *rot A*], 11.0 [CH_3 , *rot B*]. HR-ESI(+)-MS m/z calcd for $\text{C}_{23}\text{H}_{29}\text{FN}_4\text{O}$: 397.2398 [$\text{M}+\text{H}$] $^+$, found 397.2389.

2-(2-(4-(3-Fluoropropyl)phenyl)-5,7-dimethylpyrazolo[1,5-a]pyrimidin-3-yl)-N,N-dipropylacetamide (10). This amide was prepared following the general procedure described above document using 150 mg of the ester **7** (0.41 mmol), 225 μ L of *N,N*-dipropylamine (4 eq, 1.64 mmol), 810 μ L of 2.0 M trimethylaluminium solution in toluene (4 eq, 1.64 mmol), and heating at 100 °C for 1 h. **10** (105 mg, 61 %) was obtained as a beige solid after flash chromatography on silica gel (dichloromethane/methanol 99/1). R_f (dichloromethane/methanol 97/3): 0.25. t_R (HPLC A) = 1.55 min (purity: 95.4 %). Mp: 82-84 °C. ^1H NMR (CDCl_3) δ 7.76 (d, $J = 8.0$ Hz, 2H), 7.28 (d, $J = 8.0$ Hz, 2H), 6.52 (s, 1H), 4.48 (dt, $J_{\text{HF}}^2 = 47.2$ Hz, $J_{\text{HH}}^3 = 6.0$ Hz, 2H), 3.95 (s, 2H), 3.38 (t, $J = 7.6$ Hz, 2H), 3.31 (t, $J = 7.6$ Hz, 2H), 2.80 (t, $J = 7.6$ Hz, 2H), 2.75 (s, 3H), 2.55 (s, 3H), 2.04 (dtt, $J_{\text{HF}}^3 = 25.2$ Hz, $J_{\text{HH}}^3 = 7.6$ & 6.0 Hz, 2H), 1.65 (sex, $J = 7.6$ Hz, 2H), 1.55 (sex, $J = 7.6$ Hz, 2H), 0.91 (t, $J = 7.6$ Hz, 3H), 0.86 (t, $J = 7.6$ Hz, 3H). ^{13}C NMR (CDCl_3) δ 170.4 [C], 157.4 [C],

155.0 [C], 147.5 [C], 144.8 [C], 141.2 [C], 131.5 [C], 128.7 [2xCH], 128.6 [2xCH], 108.2 [CH], 101.1 [C], 83.0 [d, $J_{CF}^1 = 164$ Hz, CH₂], 49.9 [CH₂], 48.0 [CH₂], 31.9 [d, $J_{CF}^2 = 19$ Hz, CH₂], 31.0 [d, $J_{CF}^3 = 5$ Hz, CH₂], 28.1 [CH₂], 24.5 [CH₃], 22.2 [CH₂], 20.8 [CH₂], 16.8 [CH₃], 11.3 [CH₃], 11.2 [CH₃]. HR-ESI(+)-MS m/z calcd for C₂₅H₃₃FN₄O: 425.2711 [M+H]⁺, found 425.2720.

***N*-Cyclopropyl-2-(2-(4-(3-fluoropropyl)phenyl)-5,7-dimethylpyrazolo[1,5-*a*]pyrimidin-3-yl)acetamide (11).** This amide was prepared following the general procedure described above using 50 mg of the ester **7** (0.135 mmol), 38 μ L of *N*-cyclopropylamine (4 eq, 0.548 mmol), 274 μ L of 2.0 M trimethylaluminium solution in toluene (4 eq, 0.548 mmol), and heating for 45 min. **11** (42 mg, 81 %) was obtained as a white solid after trituration in cold diethyl ether. *R_f* (dichloromethane/methanol 95/5): 0.28. *t_R* (HPLC A) = 1.18 min (purity: 100.0 %). Mp: 174-176 °C. ¹H NMR (CDCl₃) δ 7.81 (d, *J* = 8.0 Hz, 2H), 7.33 (d, *J* = 8.0 Hz, 2H), 6.88 (b, *w*_{1/2} = 21 Hz, 1H), 6.60 (s, 1H), 4.48 (dt, $J_{HF}^2 = 47.2$ Hz, $J_{HH}^3 = 6.0$ Hz, 2H), 3.80 (s, 2H), 2.81 (t, *J* = 7.6 Hz, 2H), 2.79 (s, 3H), 2.65 (m, 1H), 2.60 (s, 3H), 2.05 (dtt, $J_{HF}^3 = 25.2$ Hz, $J_{HH}^3 = 7.6$ & 6.0 Hz, 2H), 0.68 (q, *J* = 6.8 Hz, 2H), 0.33 (bt, *w*_{1/2} = 21 Hz, 2H). ¹³C NMR (CDCl₃) δ 172.6 [C], 158.1 [C], 155.0 [C], 147.2 [C], 145.5 [C], 141.8 [C], 130.4 [C], 128.9 [2xCH], 128.8 [2xCH], 108.5 [CH], 100.1 [C], 83.0 [d, $J_{CF}^1 = 164$ Hz, CH₂], 31.9 [d, $J_{CF}^2 = 20$ Hz, CH₂], 31.7 [CH₂], 31.1 [d, $J_{CF}^3 = 5$ Hz, CH₂], 24.4 [CH], 22.5 [CH₃], 16.9 [CH₃], 6.3 [2xCH₂]. HR-ESI(+)-MS m/z calcd for C₂₂H₂₅FN₄O: 381.2085 [M+H]⁺, found 381.2089.

***N*-Cyclopropyl-2-(2-(4-(3-fluoropropyl)phenyl)-5,7-dimethylpyrazolo[1,5-*a*]pyrimidin-3-yl)-*N*-methylacetamide (12).** *Note: The general procedure described above failed to generate the desired amide in acceptable amount and purity. The following alternative pathway was thus used.* To a solution of **25** (277 mg, 0.81 mmol) in dichloromethane (5 mL), were added successively **24** (66 mg, 0.62 mmol), TBTU (260 mg, 0.81 mmol) and DIPEA (1.08 mL, 6.2 mmol). The reaction mixture was stirred at room temperature for 4 h. Then, it was partitioned between water and dichloromethane. The aqueous layer was extracted with dichloromethane (3 x 15 mL). The combined organic layers were washed with a 1 M hydrochloric acid aqueous solution (20 mL), brine (20 mL), dried over sodium sulfate and concentrated to dryness. The crude was purified on silica gel chromatography (toluene/acetone 80/20 to 70/30) to afford **12** as a pale yellow oil (40 mg, 15 %). *R_f* (toluene/acetone 50/50): 0.53. *t_R* (HPLC A) = 1.35 min (purity: 70.0 %). ¹H NMR (CDCl₃, 400 MHz) δ 7.73 (d, 2H, *J* = 8.8 Hz), 7.28 (d, 2H, *J* = 8.8 Hz), 6.51 (s, 1H), 4.47 (dt, 2H, $J_{HF}^2 = 45.2$ Hz, $J_{HH}^3 = 6.0$ Hz), 4.13 (s, 2H), 2.95 (s, 3H), 2.88-2.86 (m, 1H), 2.79 (t, 2H, *J* = 7.6 Hz), 2.74 (s, 3H), 2.54 (s, 3H), 2.03 (m, 2H, $J_{HF}^3 = 18.3$ Hz), 0.91-0.85 (m, 4H). ¹³C NMR (CDCl₃, 100 MHz) δ 173.8 [C], 157.4 [C], 155.0 [C], 147.6 [C], 144.6 [C], 141.1 [C], 131.6 [C], 128.6 [4 x CH], 108.2 [CH], 101.1 [C], 83.0 [d, $J_{CF}^1 = 163$ Hz, CH₂], 34.2 [CH], 31.9 [d, $J_{CF}^2 = 19$ Hz, CH₂], 31.3 [CH₃], 31.0 [d, $J_{CF}^3 = 5$ Hz, CH₂], 28.8 [CH₂], 24.6 [CH₃], 16.8 [CH₃], 9.26 [2xCH₂].

1-(Azetidin-1-yl)-2-(2-(4-(3-fluoropropyl)phenyl)-5,7-dimethylpyrazolo[1,5-*a*]pyrimidin-3-yl)ethanone (13). This amide was prepared following the general procedure described above using 150 mg of the ester **7** (0.406 mmol), 110 μ L of azetidine (4 eq, 1.63 mmol), 609 μ L of 2.0 M trimethylaluminium solution in toluene (3 eq, 1.22 mmol), and heating at 70 °C for 1 h. No acidic treatment was made for the work up of this reaction. **13** (75 mg, 49 %) was obtained as a beige powder after trituration in cold diethyl ether. *R_f* (dichloromethane/methanol 96/4): 0.18. *t_R* (HPLC A) = 1.19 min (purity: 100.0 %). Mp: 163-164 °C. ¹H NMR (CDCl₃) δ 7.77 (d, *J* = 8.0 Hz, 2H), 7.24 (d, *J* = 8.0 Hz, 2H), 6.46 (s, 1H), 4.41 (dt, $J_{HF}^2 = 47.2$ Hz, $J_{HH}^3 = 6.0$ Hz, 2H), 4.20 (t, *J* = 7.6 Hz, 2H), 3.97 (t, *J* = 7.6 Hz, 2H), 3.63 (s, 2H), 2.73 (t, *J* = 7.6 Hz, 2H), 2.67 (s, 3H), 2.49 (s, 3H), 2.17 (q⁵, *J* = 7.6 Hz, 2H), 2.04 (dtt, $J_{HF}^3 = 25.2$ Hz, $J_{HH}^3 = 7.6$ & 6.0 Hz, 2H). ¹³C NMR (CDCl₃) δ 171.0 [C], 157.6 [C], 155.2 [C], 147.4 [C], 144.8 [C], 141.3 [C], 131.3 [C], 128.8 [2xCH], 128.7 [2xCH], 108.3 [CH], 100.0 [C], 83.0 [d, $J_{CF}^1 = 164$ Hz, CH₂], 50.7 [CH₂], 48.1 [CH₂], 31.9 [d, $J_{CF}^2 = 20$ Hz, CH₂], 31.1 [d, $J_{CF}^3 = 5$ Hz, CH₂], 26.4 [CH₂], 24.6 [CH₃], 16.8 [CH₃], 15.1 [CH₂]. HR-ESI(+)-MS m/z calcd for C₂₂H₂₅FN₄O: 381.2085 [M+H]⁺, found 381.2093.

2-(2-(4-(3-Fluoropropyl)phenyl)-5,7-dimethylpyrazolo[1,5-a]pyrimidin-3-yl)-1-(pyrrolidin-1-yl)ethanone (14). This amide was prepared following the general procedure described above using 150 mg of the ester **7** (0.406 mmol), 136 μ L of pyrrolidine (4 eq, 1.63 mmol), 710 μ L of 2.0 M trimethylaluminium solution in toluene (3.5 eq, 1.42 mmol), and heating for 1 h. **14** (107 mg, 67 %) was obtained as white shiny foam after flash chromatography on silica gel (dichloromethane/methanol 99/1 to 97/3). R_f (dichloromethane/methanol 95/5): 0.29. t_R (HPLC A) = 1.27 min (purity: 100.0 %). Mp: 156-159 °C. ^1H NMR (CDCl_3) δ 7.79 (d, J = 8.0 Hz, 2H), 7.29 (d, J = 8.0 Hz, 2H), 6.52 (s, 1H), 4.47 (dt, J_{HF}^2 = 47.2 Hz, J_{HH}^3 = 6.0 Hz, 2H), 3.88 (s, 2H), 3.65 (t, J = 6.8 Hz, 2H), 3.50 (t, J = 6.8 Hz, 2H), 2.79 (t, J = 7.6 Hz, 2H), 2.74 (s, 3H), 2.54 (s, 3H), 2.03 (dt, J_{HF}^3 = 26.8 Hz, J_{HH}^3 = 7.6 & 6.0 Hz, 2H), 1.99 (q^5 , J = 6.8 Hz, 2H), 1.86 (q^5 , J = 6.8 Hz, 2H). ^{13}C NMR (CDCl_3) δ 169.4 [C], 157.5 [C], 155.2 [C], 147.5 [C], 144.8 [C], 141.2 [C], 131.5 [C], 128.8 [2xCH], 128.6 [2xCH], 108.2 [CH], 100.6 [C], 83.0 [d, J_{CF}^1 = 164 Hz, CH_2], 46.8 [CH_2], 45.9 [CH_2], 31.9 [d, J_{CF}^2 = 19 Hz, CH_2], 31.0 [d, J_{CF}^3 = 5 Hz, CH_2], 29.5 [CH_2], 26.2 [CH_2], 24.6 [CH_3], 24.4 [CH_2], 16.8 [CH_3]. HR-ESI(+)-MS m/z calcd for $\text{C}_{23}\text{H}_{27}\text{FN}_4\text{O}$: 395.2242 [M+H] $^+$, found 395.2252.

2-(2-(4-(3-Fluoropropyl)phenyl)-5,7-dimethylpyrazolo[1,5-a]pyrimidin-3-yl)-1-(piperidin-1-yl)ethanone (15). This amide was prepared following the general procedure described above using 150 mg of the ester **7** (0.406 mmol), 160 μ L of piperidine (4 eq, 1.62 mmol), 710 μ L of 2.0 M trimethylaluminium solution in toluene (3.5 eq, 1.42 mmol), and heating for 2 h. **15** (101 mg, 61 %) was obtained as beige crystals after trituration in cold diethyl ether. R_f (dichloromethane/methanol 96/4): 0.34. t_R (HPLC A) = 1.38 min (purity: 100.0 %). Mp: 145-146 °C. ^1H NMR (CDCl_3) δ 7.76 (d, J = 8.0 Hz, 2H), 7.29 (d, J = 8.0 Hz, 2H), 6.52 (s, 1H), 4.47 (dt, J_{HF}^2 = 47.2 Hz, J_{HH}^3 = 6.0 Hz, 2H), 3.95 (s, 2H), 3.57 (bs, $w_{1/2}$ = 18 Hz, 4H), 2.79 (t, J = 7.6 Hz, 2H), 2.75 (s, 3H), 2.55 (s, 3H), 2.03 (dt, J_{HF}^3 = 25.2 Hz, J_{HH}^3 = 7.6 & 6.0 Hz, 2H), 1.64-1.63 (m, $w_{1/2}$ = 18 Hz, 2H), 1.53-1.52 (m, $w_{1/2}$ = 18 Hz, 4H). ^{13}C NMR (CDCl_3) δ 169.1 [C], 157.5 [C], 155.0 [C], 147.5 [C], 144.8 [C], 141.2 [C], 131.5 [C], 128.7 [2xCH], 128.6 [2xCH], 108.3 [CH], 100.8 [C], 83.0 [d, J_{CF}^1 = 164 Hz, CH_2], 46.9 [CH_2], 43.1 [CH_2], 31.9 [d, J_{CF}^2 = 20 Hz, CH_2], 31.0 [d, J_{CF}^3 = 6.0 Hz, CH_2], 28.1 [CH_2], 26.4 [CH_2], 25.6 [CH_2], 24.6 [CH_3], 24.5 [CH_2], 16.9 [CH_3]. HR-ESI(+)-MS m/z calcd for $\text{C}_{24}\text{H}_{29}\text{FN}_4\text{O}$: 409.2398[M+H] $^+$, found 409.2393.

2-(2-(4-(3-Fluoropropyl)phenyl)-5,7-dimethylpyrazolo[1,5-a]pyrimidin-3-yl)-1-morpholinoethanone (16). This amide was prepared following the general procedure described above using 100 mg of the ester **7** (0.271 mmol), 94 mg of morpholine (4 eq, 1.08 mmol), 540 μ L of 2.0 M trimethylaluminium solution in toluene (4 eq, 1.08 mmol), and heating at 100 °C for 1 h. **16** (89 mg, 80 %) was obtained as an ocher solid after flash chromatography on silica gel (dichloromethane/methanol 99/1 to 97/3). R_f (dichloromethane/methanol 95/5): 0.33. t_R (HPLC A) = 1.15 min (purity: 95.6 %). Mp: 118-120 °C. ^1H NMR (CDCl_3) δ 7.80 (d, J = 8.0 Hz, 2H), 7.31 (d, J = 8.0 Hz, 2H), 6.54 (s, 1H), 4.48 (dt, J_{HF}^2 = 47.2 Hz, J_{HH}^3 = 5.6 Hz, 2H), 3.95 (s, 2H), 3.75-3.60 (m, 8H), 2.80 (t, J = 7.2 Hz, 2H), 2.76 (s, 3H), 2.56 (s, 3H), 2.04 (dt, J_{HF}^3 = 25.2 Hz, J_{HH}^3 = 7.2 & 5.6 Hz, 2H). ^{13}C NMR (CDCl_3) δ 169.7 [C], 157.6 [C], 155.0 [C], 147.3 [C], 144.9 [C], 141.4 [C], 131.3 [C], 128.8 [2xCH], 128.7 [2xCH], 108.4 [CH], 100.2 [C], 83.0 [d, J_{CF}^1 = 164 Hz, CH_2], 66.9 [CH_2], 66.7 [CH_2], 46.4 [CH_2], 42.3 [CH_2], 31.9 [d, J_{CF}^2 = 19 Hz, CH_2], 31.1 [d, J_{CF}^3 = 5 Hz, CH_2], 27.9 [CH_2], 24.6 [CH_3], 16.9 [CH_3]. HR-ESI(+)-MS m/z calcd for $\text{C}_{23}\text{H}_{27}\text{FN}_4\text{O}_2$: 411.2191[M+H] $^+$, found 411.2187.

2-(2-(4-(3-Fluoropropyl)phenyl)-5,7-dimethylpyrazolo[1,5-a]pyrimidin-3-yl)-1-(piperazin-1-yl)ethanone (17). This amide was prepared following the general procedure described above using 150 mg of the ester **7** (0.406 mmol), 140 mg of piperazine (4 eq, 1.63 mmol), 710 μ L of 2.0 M trimethylaluminium solution in toluene (3.5 eq, 1.42 mmol), and heating for 1 h. A basic treatment was used as work up. The reaction mixture was quenched with a 1.0 M sodium bicarbonate aqueous solution (10 mL) and the resulting inorganic precipitate was filtered off on a Büchner funnel. The filtrate was extracted as described in the general procedure. The residue was purified by flash chromatography on silica gel (dichloromethane/methanol 97/3 to 94/6) to afford **17** (141 mg, 85 %) as a pale yellow solid. R_f (dichloromethane/methanol 80/20): 0.36. t_R (HPLC A) = 0.69 min (purity: 98.5 %). Mp: 69-70 °C. ^1H NMR

(CDCl₃) δ 7.78 (d, J = 8.4 Hz, 2H), 7.30 (d, J = 8.4 Hz, 2H), 6.53 (s, 1H), 4.48 (dt, J^2_{HF} = 47.2 Hz, J^3_{HH} = 6.0 Hz, 2H), 3.94 (s, 2H), 3.66 (t, J = 4.8 Hz, 2H), 3.62 (t, J = 4.8 Hz, 2H), 2.85-2.82 (m, 4H), 2.80 (bt, 2H, J = 7.6 Hz), 2.75 (s, 3H), 2.55 (s, 3H), 2.04 (dtt, J^3_{HF} = 27.2 Hz, J^3_{HH} = 7.6 & 6.0 Hz, 2H), 1.96 (s, 1H). ¹³C NMR (CDCl₃) δ 169.5 [C], 157.7 [C], 155.0 [C], 147.3 [C], 144.9 [C], 141.4 [C], 131.2 [C], 128.8 [2xCH], 128.7 [2xCH], 108.4 [CH], 100.2 [C], 83.0 [d, J^1_{CF} = 164 Hz, CH₂], 46.3 [CH₂], 45.7 [CH₂], 45.3 [CH₂], 42.2 [CH₂], 31.9 [d, J^2_{CF} = 20 Hz, CH₂], 31.0 [d, J^3_{CF} = 5 Hz, CH₂], 28.0 [CH₂], 24.6 [CH₃], 16.8 [CH₃]. HR-ESI(+)-MS m/z calcd for C₂₃H₂₇FN₄O₂: 410.2351[M+H]⁺, found 410.2358.

2-(2-(4-(3-Fluoropropyl)phenyl)-5,7-dimethylpyrazolo[1,5-*a*]pyrimidin-3-yl)-1-(piperazin-1-yl)ethanone hydrochloride (17.HCl). To a solution of **17** (28 mg, 0.068 mmol) in dichloromethane (0.50 mL) were added a few drops of a 1.25 M hydrochloric acid solution in methanol. The resulting precipitate was filtered on a Büchner funnel, washed with cold diethyl ether (4 x 2 mL) and suck-dried to afford **17.HCl** (14 mg, 46 %) as bright yellow crystals. Mp: 120-122 °C. ¹H NMR (MeOD-*d*₄) δ 7.65 (d, J = 8.0 Hz, 2H), 7.40 (d, J = 8.0 Hz, 2H), 7.15 (s, 1H), 4.47 (dt, J^2_{HF} = 47.6 Hz, J^3_{HH} = 6.0 Hz, 2H), 4.20 (s, 2H), 3.99 (bt, $w_{1/2}$ = 16 Hz, 2H), 3.89 (bt, $w_{1/2}$ = 16 Hz, 2H), 3.41 (bt, $w_{1/2}$ = 16 Hz, 2H), 3.31 (m, 2H), 2.96 (s, 3H), 2.85-2.80 (m, 5H), 2.04 (dtt, J^3_{HF} = 24.8 Hz, J^3_{HH} = 7.2 & 6.0 Hz, 2H).

***N*-Benzyl-2-(2-(4-(3-fluoropropyl)phenyl)-5,7-dimethylpyrazolo[1,5-*a*]pyrimidin-3-yl)-*N*-methylacetamide (18).** This amide was prepared following the general procedure described above using 150 mg of the ester **7** (0.406 mmol), 210 μ L of *N*-benzylmethylamine (4 eq, 1.63 mmol), 710 μ L of 2.0 M trimethylaluminium solution in toluene (3.5 eq, 1.42 mmol), and heating for 1 h. **18** (112 mg, 62 %) was obtained as an orange gum after flash chromatography on silica gel (dichloromethane/methanol 99/1) and a trituration in cold diethyl ether. R_f (dichloromethane/methanol 98/2): 0.25. t_R (HPLC A) = 1.47 min (purity: 100.0 %). ¹H NMR (CDCl₃) δ 7.78-7.74 (d, J = 7.6 Hz, 2H), 7.32-7.10 (m, 7H), 6.54 (s, 0.55H, *rot A*), 6.48 (s, 0.45H, *rot B*), 4.73 (s, 0.90H, *rot B*), 4.63 (s, 1.10 H, *rot A*), 4.48 (dt, J^2_{HF} = 47.2 Hz, J^3_{HH} = 6.0 Hz, 2H), 4.03 (s, 0.90H, *rot B*), 4.01 (s, 1.10H, *rot A*), 3.06 (s, 1.65H, *rot A*), 2.96 (s, 1.35H, *rot B*), 2.81 (t, J = 7.2 Hz, 2H), 2.76 (s, 1.65H, *rot A*), 2.70 (s, 1.35H, *rot B*), 2.56 (s, 1.65H, *rot A*), 2.54 (s, 1.35H, *rot B*), 2.04 (dtt, J^3_{HF} = 25.6 Hz, J^3_{HH} = 7.2 & 6.0 Hz, 2H). ¹³C NMR (CDCl₃) δ 171.3 [C, *rot B*], 171.0 [C, *rot A*], 157.6 [C, *rot B*], 157.4 [C, *rot A*], 155.1 [C], 147.3 [C, *rot A*], 147.5 [C, *rot B*], 144.9 [C], 141.2 [C], 137.4 [C, *rot A*], 136.7 [C, *rot B*], 131.3 [C], 128.7 [2xCH], 128.6 [2xCH], 128.5 [CH, *rot B*], 124.8 [CH, *rot A*], 128.0 [CH, *rot A*], 127.1 [CH, *rot B*], 127.1 [CH, *rot A*], 126.1 [CH, *rot B*], 108.2 [CH], 100.5 [C], 83.0 [d, J^1_{CF} = 164 Hz, CH₂], 53.5 [CH₂, *rot B*], 51.2 [CH₂, *rot A*], 35.1 [CH₃, *rot A*], 34.2 [CH₃, *rot B*], 31.9 [d, J^2_{CF} = 20 Hz, CH₂], 31.1 [CH₂], 28.4 [CH₂], 24.5 [CH₃], 16.8 [CH₃]. HR-ESI(+)-MS m/z calcd for C₂₇H₂₉FN₄O: 445.2398[M+H]⁺, found 445.2414.

2-(2-(4-(3-Fluoropropyl)phenyl)-5,7-dimethylpyrazolo[1,5-*a*]pyrimidin-3-yl)-*N*-methyl-*N*-(pyridin-3-yl)methyl)acetamide (19). This amide was prepared following the general procedure described above using 198 μ L of *N*-methyl-1-(pyridin-3-yl)methanamine (4 eq, 1.62 mmol), 710 μ L of 2 M trimethylaluminium solution in toluene (3.5 eq 1.42 mmol), 150 mg of the ester **7** (0.406 mmol) and heating for 1 h. No acidic treatment was made for the work up of this reaction. **19** was obtained as a pale yellow solid after flash chromatography on silica gel (dichloromethane/methanol 98/2 to 97/3) and trituration in cold diethyl ether (141 mg, 78 %). R_f (dichloromethane/methanol 94/4): 0.20. t_R (HPLC A) = 0.88 min (purity: 97.5 %). Mp: 149-151 °C. ¹H NMR (CDCl₃, 400 MHz) δ 8.52-8.48 (m, 2H), 7.80 (d, 0.6 H, J = 8.0 Hz, *rot B*), 7.72 (d, 1.4H, J = 8.0 Hz, *rot A*), 7.57 (d, 0.7 H, J = 8.0 Hz, *rot A*), 7.41 (d, 0.3H, J = 8.0 Hz, *rot B*), 7.31-7.20 (m, 3H), 6.54 (s, 0.7H, *rot A*), 6.48 (s, 0.3H, *rot B*), 4.74 (s, 0.6H, *rot B*), 4.62 (s, 1.4H, *rot A*), 4.48 (dt, 2H, J^2_{HF} = 47.2 Hz, J^3_{HH} = 6.0 Hz), 4.05 (s, 0.6H, *rot B*), 4.01 (s, 1.4H, *rot A*), 3.09 (s, 2.1H, *rot A*), 2.93 (s, 0.9H, *rot B*), 2.80 (t, 2H, J = 7.2 Hz), 2.75 (s, 2.1H, *rot A*), 2.68 (s, 0.9H, *rot B*), 2.55 (s, 2.1H, *rot A*), 2.54 (s, 0.9H, *rot B*), 2.04 (dtt, 2H, J^3_{HF} = 25.6 Hz, J^3_{HH} = 7.2 & 6.0 Hz). ¹³C NMR (CDCl₃, 100 MHz) δ 171.4 [C, *rot B*], 171.3 [C, *rot A*], 157.7 [C], 155.0 [C], 149.2 [CH, *rot A*], 148.7 [CH, *rot A*], 148.6 [CH, *rot B*], 147.9 [CH, *rot B*], 147.5 [C, *rot A*], 147.0 [C, *rot B*], 144.8 [C, *rot A*], 144.7 [C, *rot B*], 141.3 [C], 135.9

[CH, *rot A*], 133.6 [CH, *rot B*], 133.1 [C, *rot A*], 132.2 [C, *rot B*], 131.4 [C, *rot A*], 131.1 [C, *rot B*], 128.6 [4xCH], 123.5 [CH, *rot A*], 123.2 [CH, *rot B*], 108.3 [CH], 100.2 [C], 83.0 [d, $J_{CF}^1 = 164$ Hz, CH₂], 51.2 [CH₂, *rot A*], 48.9 [CH₂, *rot B*], 35.4 [CH₃, *rot A*], 34.2 [CH₃, *rot B*], 31.8 [d, $J_{CF}^2 = 20$ Hz, CH₂], 31.1 [CH₂], 28.7 [CH₂, *rot B*], 28.4 [CH₂, *rot A*], 24.63 [CH₃], 16.8 [CH₃]. HR-ESI(+)-MS *m/z* calcd for C₂₆H₂₈FN₅O₂: 446.2351[M+H]⁺, found 446.2346.

2-(2-(4-(3-Fluoropropyl)phenyl)-5,7-dimethylpyrazolo[1,5-a]pyrimidin-3-yl)-N-methyl-N-(2-(pyridin-2-ylmethyl)acetamide (20). This amide was prepared following the general procedure described above using 300 mg of the ester **7** (0.81 mmol), 198 mg of *N*-methyl-1-(pyridin-2-yl)methanamine (2 eq, 1.63 mmol), 163 μ L of 2 M trimethylaluminium solution in toluene (4 eq, 3.25 mmol), and heating for 5 h. **20** (110 mg, 30 %) was obtained as a light yellow foam after flash chromatography on silica gel (dichloromethane/methanol 95/5). *R_f* (dichloromethane/acetone 90/10): 0.19. *t_R* (HPLC A) = 1.07 min (purity: 96.0 %). ¹H NMR (CDCl₃, 400 MHz): δ 8.56 (m, 1H), 7.78 (d, 0.8H, *J* = 8.0 Hz, *rot B*), 7.74 (d, 1.2H, *J* = 8.0 Hz, *rot A*), 7.63-7.57 (m, 1H), 7.29-7.14 (m, 4H), 6.53 (s, 0.6H, *rot A*), 6.48 (s, 0.4H, *rot B*), 4.83 (s, 0.8H, *rot B*), 4.75 (s, 1.2H, *rot A*), 4.48 (dt, 2H, $J_{HF}^2 = 47.2$ Hz, $J_{HH}^3 = 5.6$ Hz), 4.05 (s, 1.2H, *rot B*), 4.03 (s, 1.8H, *rot A*), 3.20 (s, 1.8H, *rot A*), 3.00 (s, 1.2H, *rot B*), 2.80 (t, 2H, *J* = 7.2 Hz), 2.77 (s, 1.8H, *rot A*), 2.69 (s, 1.2H, *rot B*), 2.55 (s, 1.8H, *rot A*), 2.53 (s, 1.2H, *rot B*), 2.04 (m, 2H, $J_{HF}^2 = 25.6$ Hz). ¹³C NMR (CDCl₃, 100 MHz): δ 171.6 [C, *rot B*], 171.1 [C, *rot A*], 157.6 [C], 156.9 [C], 155.0 [C, *rot A*], 154.9 [C, *rot B*], 149.4 [CH, *rot B*], 148.9 [CH, *rot A*], 147.5 [C, *rot A*], 147.3 [C, *rot B*], 144.8 [C, *rot A*], 144.6 [C, *rot B*], 141.2 [C], 136.6 [CH], 131.4 [C, *rot A*], 131.3 [C, *rot B*], 128.7 [2xCH], 128.6 [2xCH], 122.1 [CH], 120.1 [CH], 108.3 [CH, *rot A*], 108.2 [CH, *rot B*], 100.5 [C, *rot A*], 100.3 [C, *rot B*], 82.9 [d, $J_{CF}^1 = 163$ Hz, CH₂], 55.5 [CH₂, *rot B*], 53.5 [CH₂, *rot A*], 36.1 [CH₃, *rot A*], 34.6 [CH₃, *rot B*], 31.9 [d, $J_{CF}^2 = 19$ Hz, CH₂], 31.0 [d, $J_{CF}^3 = 5$ Hz, CH₂], 28.5 [CH₂, *rot B*], 28.3 [CH₂, *rot A*], 24.5 [CH₃], 16.8 [CH₃]. HR-ESI(+)-MS *m/z* calcd for C₂₆H₂₈FN₅O₂: 446.2351 [M+H]⁺, found 446.2367

2-(2-(4-(3-Fluoropropyl)phenyl)-5,7-dimethylpyrazolo[1,5-a]pyrimidin-3-yl)-N-methyl-N-phenethylacetamide (21). This amide was prepared following the general procedure described above using 300 mg of the ester **7** (0.81 mmol), 220 mg of *N*-methylphenethylamine (2 eq, 1.63 mmol), 163 μ L of 2 M trimethylaluminium solution in toluene (4 eq, 3.25 mmol), and heating at 110 °C for 4 h. **21** (84 mg, 23 %) was obtained as pale orange solid after flash chromatography on silica gel (dichloromethane/acetone 95/5 to 80/20). *R_f* (dichloromethane/acetone 90/10): 0.19. *t_R* (HPLC A) = 1.39 min (purity: 96.4 %). Mp: 99-101 °C. ¹H NMR (CDCl₃, 400 MHz) δ 7.70-7.72 (m, 2H), 7.30-7.25 (m, 4H), 7.22-7.19 (m, 2H), 7.18-7.14 (m, 1H), 6.53 (s, 0.5H, *rot A*), 6.51 (s, 0.5H, *rot B*), 4.48 (dt, 2H, $J_{HF}^2 = 48$ Hz, $J_{HH}^3 = 6.0$ Hz), 3.92 (s, 1H, *rot A*), 3.88 (s, 1 H, *rot B*), 3.71 (t, 0.98H, *J* = 7.2 Hz, *rot B*), 3.61 (t, 1.02H, *J* = 7.2 Hz, *rot A*), 3.02 (s, 1.5H, *rot A*), 2.93 (s, 1.5H, *rot B*), 2.85-2.77 (m, 4H), 2.76 (s, 1.5H, *rot A*), 2.74 (s, 1.5H, *rot B*), 2.57 (s, 1.5H, *rot A*), 2.52 (s, 1.5H, *rot B*), 2.09-1.96 (dq⁵, 2H, $J_{HF}^3 = 26.8$ Hz, $J_{HH}^3 = 6.0$ Hz). ¹³C NMR (CDCl₃, 100 MHz) δ 170.8 [C, *rot B*], 170.5 [C, *rot A*], 157.4 [C], 155.0 [C], 174.3 [C], 144.7 [C], 141.2 [C], 139.3 [C, *rot A*], 138.3 [C, *rot B*], 131.4 [C, *rot A*], 131.3 [C, *rot B*], 128.8 [2xCH], 128.7 [2xCH], 128.6 [4xCH], 126.5 [CH, *rot B*], 126.1 [CH, *rot A*], 108.2 [CH], 100.6 [C], 82.9 [d, $J_{CF}^1 = 163.8$ Hz, CH₂], 51.9 [CH₂, *rot B*], 50.6 [CH₂, *rot A*], 36.5 [CH₃, *rot A*], 34.9 [CH₂, *rot B*], 34.1 [CH₃, *rot B*], 33.6 [CH₂, *rot A*], 31.9 [d, $J_{CF}^2 = 19.6$ Hz, CH₂], 31.0 [d, $J_{CF}^3 = 5.4$ Hz, CH₂], 28.5 [CH₂, *rot A*], 27.9 [CH₂, *rot B*], 24.5 [CH₃], 16.8 [CH₃]. HR-ESI(+)-MS *m/z* calcd for C₂₈H₃₁FN₄O: 459.2555 [M+H]⁺, found 459.2556.

***N*-Benzylcyclopropanamine (22).** To a solution of cyclopropylamine (5.0 g, 87 mmol) in tetrahydrofuran (120 mL) was added triethylamine (19 mL, 131 mmol) at ambient temperature. Benzyl bromide (12 mL, 105 mmol) was then carefully added dropwise to the reaction mixture which was stirred overnight at ambient temperature. The reaction mixture was partitioned between water and ethyl acetate. The aqueous layer was extracted twice with ethyl acetate (2 x 100 mL). The combined organic layers were washed with water (2 x 100 mL) and brine (100 mL), dried over sodium sulfate, filtered and concentrated to dryness. The residue was purified by

chromatography on silica gel (dichloromethane/methanol 100/0 to 98/2) to afford **22** (3.25 g, 49 %) as a light yellow oil. R_f (dichloromethane/methanol 96/4): 0.36. ^1H NMR (CDCl_3 , 400 MHz) δ 7.33 (m, 4H), 7.29-7.24 (m, 1H), 3.86 (s, 2H), 2.17 (m, 1H), 1.91 (s, 1H), 0.48-0.44 (m, 2H), 0.43-0.39 (m, 2H). ^{13}C NMR (CDCl_3 , 100 MHz) δ 140.5 [C], 128.4 [2xCH], 128.2 [2xCH], 126.8 [CH], 53.7 [CH_2], 30.0 [CH], 6.4 [2x CH_2].

N-Benzyl-N-methylcyclopropanamine (23). To a cooled solution (0 °C) of **22** (3.0 g, 20.3 mmol) in methanol (40 mL) was added a 37 % wt. aqueous formaldehyde solution (2.5 mL, 30.5 mmol). Sodium borohydride (1.15 g, 30.5 mmol) was cautiously added to the mixture (exothermic reaction) which was then stirred for 30 min at 0 °C. Once completed, the reaction was quenched with a saturated potassium carbonate aqueous solution (100 mL). The mixture was then extracted twice with ethyl acetate (2 x 50 mL). The organic layers were combined, washed twice with water (2 x 25 mL) and brine (25 mL), dried over sodium sulfate, filtered and concentrated to dryness. The residue was purified by chromatography on silica gel (dichloromethane/methanol 100/0 to 99/1) to afford **23** (2.45 g, 74 %) as a colorless oil. R_f (dichloromethane/methanol 95/5): 0.41. ^1H NMR (CDCl_3 , 400 MHz) δ 7.32-7.24 (m, 5H), 3.68 (s, 2H), 2.27 (s, 3H), 1.73-1.70 (m, 1H), 0.49-0.45 (m, 4H). ^{13}C NMR (CDCl_3 , 100 MHz) δ 138.4 [C], 129.3 [2xCH], 128.0 [2xCH], 126.8 [CH], 62.2 [CH_2], 41.9 [CH], 38.4 [CH_3], 7.1 [2x CH_2].

N-Methylcyclopropanamine hydrochloride (24). To a solution of **23** (417 mg, 2.59 mmol) in methanol (10 mL) was cautiously added 10 % palladium on charcoal (26 mg, 1 mol %). The reaction vessel was degassed under reduced pressure and filled with hydrogen at 1 atm (two cycles). The reaction mixture was stirred at ambient temperature overnight. Then, the catalyst was filtered off using a Celite[®] pad and washed with dichloromethane/methanol 80/20 (100 mL). A methanolic 10 M hydrochloric acid solution (3 mL) was added. The filtrate was further concentrated to dryness to afford **24** (177 mg, 63 %) as a pale yellow oil stored under argon. R_f (dichloromethane/methanol 90/10): 0.1. ^1H NMR ($\text{MeOH}-d_4$, 400 MHz) δ 2.77 (m, 4H), 0.91-0.89 (m, 4H). ^{13}C NMR ($\text{MeOH}-d_4$, 100 MHz) δ 32.5 [CH_3], 31.2 [CH], 2.6 [2x CH_2].

2-(2-(4-(3-Fluoropropyl)phenyl)-5,7-dimethylpyrazolo[1,5-a]pyrimidin-3-yl)acetic acid (25). To a solution of the ester **7** (460 mg, 1.26 mmol) in methanol (10 mL), was added potassium hydroxide (212 mg, 3.78 mmol). The reaction mixture was heated at 40 °C for 5 h. Water (5 mL) was added to quench the reaction. The reaction mixture was then acidified to pH 2 with a 1 M hydrochloric acid aqueous solution. The formed precipitate was filtered off, washed with diethyl ether, and dried under vacuum to afford **25** as a beige solid (277 mg, 64 %), that was engaged without further purification in the coupling step (see preparation of **12** above).

5.2. Binding studies

Binding affinities for the TSPO (K_i) were determined using membrane homogenates from rat heart and screened against [^3H]PK11195 ($K_d = 1.8$ nM, $c = 0.2$ nM). Affinities for the CBR were determined at a unique concentration (1 μM), using membrane homogenates from rat cerebral cortex and screened against [^3H]flunitrazepam ($K_d = 2.1$ nM, $c = 0.4$ nM). This work was done by CEREP (<http://www.cerep.fr>).

5.3. LogD_{7.4} / clogP determination, and TPSA calculation

LogD_{7.4} (*n*-octanol/buffer pH 7.4 partition coefficient) values were determined based on a validated and standardized HPLC method (HPLC B), by conversion of the recorded retention time for each compound (correlation between retention times and known logD values of similar compounds). Calculated LogP (cLogP) as well as topological polar surface area (TPSA, expressed in Å²) were determined using ChemDraw Professional 15.0 (Cambridge Soft., PerkinElmer, Waltham, MA, USA).

5.4. Microsomal metabolic stability evaluation

Compounds were incubated with hepatic microsomal fractions (male CD1 mouse, male Sprague-Dawley rat or humans (BD pool)) using the following experimental conditions throughout the study: microsomal proteins concentration = 0.25 mg/mL; substrate concentration = 0.5 μM; cofactor = 1 mM NADPH. For each compound to be tested, 5 samples were prepared, and incubated respectively for 0, 5, 10, 20 and 30 min. Enzyme activity was stopped with 1 volume of CH₃CN, and proteins removed by centrifugation. The supernatant fluids were then analysed by UPLC/HRMS (UPLC: Polaris C18 (50 x 2.0 mm, 3 μm) column (Agilent, Santa Clara, CA, USA); mobile phase: (A) H₂O + 0.1% formic acid, (B) CH₃CN + 0.1% formic acid; gradient (A/B): 90:10 to 10:90 (2.1 min), then 10:90 for 0.3 min and back to 90:10 (0.1 min) ; 0.5 mL/min; injection volume: 5 μL. HRMS: Thermo Scientific Hybride Q Exactive™ quadripôle-Orbitrap (Thermo Fisher Scientific, Inc., NYSE:TMO, Waltham, MA, USA)). The data were collected and processed using GMSU software (GUBBS, Alpharetta, GA, USA), leading to quantification of the unchanged tested compound. Intrinsic clearances were expressed as μL / min / mg protein, and calculated, for each compound, as below.

First, the percentage of unchanged compound (% stability) at T = 5, 10, 20 and 30 min was calculated by normalizing the data at these time points to the data recorded at T = 0 min for the analyte / internal standard peak area ratio. % stability = [peak area ratio at T / peak area ratio at T₀] x 100. Then, the elimination slope (-k) (k is expressed in min⁻¹) was determined using a linear regression of the neperian logarithm (ln) of the % stability versus the incubation time (T). Finally, intrinsic clearance (InC) was determined as follows: InC = [k / protein concentration] x 1000 (protein concentration is expressed in mg / mL).

Acknowledgments

This work was supported by CEA-I²BM intramural programs, as well as partly by the European Union's Seventh Framework Programme [FP7/2007-2013] INMiND (Grant agreement n° HEALTH-F2-2011-278850) and France Life Imaging (Grant agreement n° ANR-11-INBS-0006). The authors wish to thank LGCR Analytical Sciences (Sanofi, Chilly Mazarin) for logD_{7.4} measurements, DMPK (Sanofi, Montpellier) and DSAR Drug Disposition (Sanofi, Vitry) for preliminary metabolism studies. HRMS determination has benefited from the facilities and expertise of scientific service, HPLC-Mass spectrometry of ICSN, CNRS, Gif sur Yvette, France (www.icsn.cnrs-gif.fr).

References

- [1] V. Papadopoulos, M. Baraldi, T.R. Guilarte, T.B. Knudsen, J.-J. Lacapère, P. Lindemann, M.D. Norenberg, D. Nutt, A. Weizman, M.-R. Zhang, M. Gavish, Translocator protein (18kDa): new nomenclature for the peripheral-type benzodiazepine receptor based on its structure and molecular function, *Trends Pharmacol. Sci.* 27 (2006) 402–409. doi:10.1016/j.tips.2006.06.005.
- [2] P. Casellas, S. Galiegue, A.S. Basile, Peripheral benzodiazepine receptors and mitochondrial function, *Neurochem. Int.* 40 (2002) 475–486. doi:10.1016/S0197-0186(01)00118-8.

- [3] V. Papadopoulos, H. Amri, N. Boujrad, C. Cascio, M. Culty, M. Garnier, M. Hardwick, H. Li, B. Vidic, A.S. Brown, J.L. Reversa, J.M. Bernassau, K. Drieu, Peripheral benzodiazepine receptor in cholesterol transport and steroidogenesis, *Steroids*. 62 (1997) 21–28. doi:10.1016/S0039-128X(96)00154-7.
- [4] R. Rupprecht, V. Papadopoulos, G. Rammes, T.C. Baghai, J. Fan, N. Akula, G. Groyer, D. Adams, M. Schumacher, Translocator protein (18 kDa) (TSPO) as a therapeutic target for neurological and psychiatric disorders, *Nat. Rev. Drug Discov.* 9 (2010) 971–988. doi:10.1038/nrd3295.
- [5] C.J.D. Austin, J. Kahlert, M. Kassiou, L.M. Rendina, The translocator protein (TSPO): A novel target for cancer chemotherapy, *Int. J. Biochem. Cell Biol.* 45 (2013) 1212–1216. doi:10.1016/j.biocel.2013.03.004.
- [6] E.L. Werry, M.L. Barron, M. Kassiou, TSPO as a target for glioblastoma therapeutics, *Biochem. Soc. Trans.* 43 (2015) 531–536. doi:10.1042/BST20150015.
- [7] S.W. Chua, M. Kassiou, L.M. Ittner, The translocator protein as a drug target in Alzheimer's disease, *Expert Rev. Neurother.* 14 (2014) 439–448. doi:10.1586/14737175.2014.896201.
- [8] S. Venneti, B.J. Lopresti, C.A. Wiley, The peripheral benzodiazepine receptor (Translocator protein 18 kDa) in microglia: From pathology to imaging, *Prog. Neurobiol.* 80 (2006) 308–322. doi:10.1016/j.pneurobio.2006.10.002.
- [9] A.M. Scarf, M. Kassiou, The translocator protein, *J. Nucl. Med.* 52 (2011) 677–680. doi:10.2967/jnumed.110.086629.
- [10] C. Luus, R. Hanani, A. Reynolds, M. Kassiou, The development of PET radioligands for imaging the translocator protein (18 kDa): What have we learned?, *J. Label. Compd. Radiopharm.* 53 (2010) 501–510. doi:10.1002/jlcr.1752.
- [11] A.M. Scarf, L.M. Ittner, M. Kassiou, The translocator protein (18 kDa): central nervous system disease and drug design, *J. Med. Chem.* 52 (2009) 581–592. doi:10.1021/jm8011678.
- [12] F. Dollé, C. Luus, A. Reynolds, M. Kassiou, Radiolabelled molecules for imaging the Translocator Protein (18 kDa) using Positron Emission Tomography, *Curr. Med. Chem.* 16 (2009) 2899–2923. doi:10.2174/092986709788803150.
- [13] S. Taliani, I. Pugliesi, F. Da Settimo, Structural requirements to obtain highly potent and selective 18 kDa Translocator Protein (TSPO) Ligands, *Curr. Top. Med. Chem.* 11 (2011) 860–886. doi:10.2174/156802611795165142.
- [14] A.M. Scarf, C. Luus, E. Da Pozzo, S. Selleri, C. Guarino, C. Martini, L.M. Ittner, M. Kassiou, Evidence for complex binding profiles and species differences at the translocator protein (TSPO) (18 kDa), *Curr. Mol. Med.* 12 (2012) 488–493.
- [15] R.B. Banati, J. Newcombe, R.N. Gunn, A. Cagnin, F. Turkheimer, F. Heppner, G. Price, F. Wegner, G. Giovannoni, D.H. Miller, G.D. Perkin, T. Smith, A.K. Hewson, G. Bydder, G.W. Kreutzberg, T. Jones, M.L. Cuzner, R. Myers, The peripheral benzodiazepine binding site in the brain in multiple sclerosis, *Brain*. 123 (2000) 2321–2337. doi:10.1093/brain/123.11.2321.
- [16] B. Ferzaz, E. Brault, G. Bourliand, J.-P. Robert, G. Poughon, Y. Claustre, F. Marguet, P. Liere, M. Schumacher, J.-P. Nowicki, J. Fournier, B. Marabout, M. Sevrin, P. George, P. Soubrie, J. Benavides, B. Scatton, SSR180575 (7-Chloro-N,N,5-trimethyl-4-oxo-3-phenyl-3,5-dihydro-4H-pyridazino[4,5-b]indole-1-acetamide), a Peripheral Benzodiazepine Receptor ligand, promotes neuronal survival and repair, *J. Pharmacol. Exp. Ther.* 301 (2002) 1067–1078. doi:10.1124/jpet.301.3.1067.
- [17] N. Leducq, F. Bono, T. Sulpice, V. érie Vin, P. Janiak, G.L. Fur, S.E. O'Connor, J.-M. Herbert, Role of peripheral benzodiazepine receptors in mitochondrial, cellular, and cardiac damage induced by oxidative Stress and ischemia-reperfusion, *J. Pharmacol. Exp. Ther.* 306 (2003) 828–837. doi:10.1124/jpet.103.052068.
- [18] C. Thominiaux, A. Damont, B. Kuhnast, S. Demphel, S. Le Helleix, S. Boisnard, L. Rivron, F. Chauveau, H. Boutin, N. Van Camp, R. Boisgard, S. Roy, J. Allen, T. Rooney, J. Benavides, P. Hantraye, B. Tavitian, F. Dollé, Radiosynthesis of 7-chloro-N,N-dimethyl-5-[¹¹C]methyl-4-oxo-3-phenyl-3,5-dihydro-4H-pyridazino[4,5-b]indole-1-acetamide, [¹¹C]SSR180575, a novel radioligand for imaging the TSPO (peripheral benzodiazepine receptor) with PET, *J. Label. Compd. Radiopharm.* 53 (2010) 767–773. doi:10.1002/jlcr.1794.

- [19] F. Chauveau, H. Boutin, N. Van Camp, C. Thominiaux, P. Hantraye, L. Rivron, F. Marguet, M.-N. Castel, T. Rooney, J. Benavides, F. Dollé, B. Tavitian, In vivo imaging of neuroinflammation in the rodent brain with [11C]SSR180575, a novel indoleacetamide radioligand of the translocator protein (18 kDa), *Eur. J. Nucl. Med. Mol. Imaging.* 38 (2011) 509–514. doi:10.1007/s00259-010-1628-5.
- [20] N. Van Camp, S. Lavis, L. Rbah, R. Aaron-Badin, C. Jan, F. Dollé, T. Rooney, E. Brouillet, P. Hantraye, 11C-SSR180575 evaluated under normal and pathological conditions in nonhuman primate brain., *J. Nucl. Med.* 53 Suppl. 1 (2012) 109P.
- [21] Y.-Y. Cheung, M.L. Nickels, D. Tang, J.R. Buck, H.C. Manning, Facile synthesis of SSR180575 and discovery of 7-chloro-N,N,5-trimethyl-4-oxo-3(6-[18F]fluoropyridin-2-yl)-3,5-dihydro-4H-pyridazino[4,5-b]indole-1-acetamide, a potent pyridazinoindole ligand for PET imaging of TSPO in cancer, *Bioorg. Med. Chem. Lett.* 24 (2014) 4466–4471. doi:10.1016/j.bmcl.2014.07.091.
- [22] A. Damont, F. Marguet, F. Puech, F. Dollé, Synthesis and in vitro characterization of novel fluorinated derivatives of the TSPO 18 kDa ligand SSR180575, *Eur. J. Med. Chem.* 101 (2015) 736–745. doi:10.1016/j.ejmech.2015.07.033.
- [23] H. Boutin, F. Chauveau, C. Thominiaux, B. Kuhnast, M.-C. Grégoire, S. Jan, R. Trebossen, F. Dollé, B. Tavitian, F. Mattner, A. Katsifis, In vivo imaging of brain lesions with [11C]CLINME, a new PET radioligand of peripheral benzodiazepine receptors, *Glia.* 55 (2007) 1459–1468. doi:10.1002/glia.20562.
- [24] C. Thominiaux, F. Mattner, I. Greguric, H. Boutin, F. Chauveau, B. Kuhnast, M.-C. Grégoire, C. Loc'h, H. Valette, M. Bottlaender, P. Hantraye, B. Tavitian, A. Katsifis, F. Dollé, Radiosynthesis of 2-[6-chloro-2-(4-iodophenyl)imidazo[1,2-a]pyridin-3-yl]-N-ethyl-N-[11C]methyl-acetamide, [11C]CLINME, a novel radioligand for imaging the peripheral benzodiazepine receptors with PET, *J. Label. Compd. Radiopharm.* 50 (2007) 229–236. doi:10.1002/jlcr.1258.
- [25] C.J.R. Fookes, T.Q. Pham, F. Mattner, I. Greguric, C. Loc'h, X. Liu, P. Berghofer, R. Shepherd, M.-C. Grégoire, A. Katsifis, Synthesis and biological evaluation of substituted [18F]imidazo[1,2-a]pyridines and [18F]pyrazolo[1,5-a]pyrimidines for the study of the peripheral benzodiazepine receptor using Positron Emission Tomography, *J. Med. Chem.* 51 (2008) 3700–3712. doi:10.1021/jm7014556.
- [26] F. Dollé, F. Hinnen, A. Damont, B. Kuhnast, C. Fookes, T. Pham, B. Tavitian, A. Katsifis, Radiosynthesis of [18F]PBR111, a selective radioligand for imaging the translocator protein (18 kDa) with PET, *J. Label. Compd. Radiopharm.* 51 (2008) 435–439. doi:10.1002/jlcr.1559.
- [27] T. Bourdier, T.Q. Pham, D. Henderson, T. Jackson, P. Lam, M. Izard, A. Katsifis, Automated radiosynthesis of [18F]PBR111 and [18F]PBR102 using the Tracerlab FXFN and Tracerlab MXFDG module for imaging the peripheral benzodiazepine receptor with PET, *Appl. Radiat. Isot.* 70 (2012) 176–183. doi:10.1016/j.apradiso.2011.07.014.
- [28] S. Dedeurwaerdere, P.D. Callaghan, T. Pham, G.L. Rahardjo, H. Amhaoul, P. Berghofer, M. Quinlivan, F. Mattner, C. Loc'h, A. Katsifis, M.-C. Grégoire, PET imaging of brain inflammation during early epileptogenesis in a rat model of temporal lobe epilepsy, *EJNMMI Res.* 2 (2012) 60. doi:10.1186/2191-219X-2-60.
- [29] J.D. Verschuer, J. Towson, S. Eberl, A. Katsifis, D. Henderson, P. Lam, L. Wen, C. Loc'h, F. Mattner, S. Thomson, A. Mohamed, M.J. Fulham, Radiation dosimetry of the translocator protein ligands [18F]PBR111 and [18F]PBR102, *Nucl. Med. Biol.* 39 (2012) 742–753. doi:10.1016/j.nucmedbio.2011.11.003.
- [30] F. Mattner, A. Katsifis, M. Staykova, P. Ballantyne, D.O. Willenborg, Evaluation of a radiolabelled peripheral benzodiazepine receptor ligand in the central nervous system inflammation of experimental autoimmune encephalomyelitis: a possible probe for imaging multiple sclerosis, *Eur. J. Nucl. Med. Mol. Imaging.* 32 (2004) 557–563. doi:10.1007/s00259-004-1690-y.
- [31] N. Arlicot, A. Katsifis, L. Garreau, F. Mattner, J. Vergote, S. Duval, S. Bodard, D. Guilloteau, S. Chalon, Evaluation of CLINDE as potent translocator protein (18 kDa) SPECT radiotracer reflecting the degree of neuroinflammation in a rat model of microglial activation, *Eur. J. Nucl. Med. Mol. Imaging.* 35 (2008) 2203–2211. doi:10.1007/s00259-008-0834-x.

- [32] F. Mattner, D.L. Bandin, M. Staykova, P. Berghofer, M.C. Gregoire, P. Ballantyne, M. Quinlivan, S. Fordham, T. Pham, D.O. Willenborg, A. Katsifis, Evaluation of [¹²³I]-CLINDE as a potent SPECT radiotracer to assess the degree of astroglia activation in cuprizone-induced neuroinflammation, *Eur. J. Nucl. Med. Mol. Imaging.* 38 (2011) 1516–1528. doi:10.1007/s00259-011-1784-2.
- [33] F. Mattner, K. Mardon, A. Katsifis, Pharmacological evaluation of [¹²³I]-CLINDE: a radioiodinated imidazopyridine-3-acetamide for the study of peripheral benzodiazepine binding sites (PBBS), *Eur. J. Nucl. Med. Mol. Imaging.* 35 (2007) 779–789. doi:10.1007/s00259-007-0645-5.
- [34] Q. Guo, A. Colasanti, D.R. Owen, M. Onega, A. Kamalakaran, I. Bennacef, P.M. Matthews, E.A. Rabiner, F.E. Turkheimer, R.N. Gunn, Quantification of the specific translocator protein signal of 18F-PBR111 in healthy humans: A genetic polymorphism effect on in vivo binding, *J. Nucl. Med.* 54 (2013) 1915–1923. doi:10.2967/jnumed.113.121020.
- [35] L. Feng, C. Svarer, G. Thomsen, R. de Nijs, V.A. Larsen, P. Jensen, D. Adamsen, A. Dyssegaard, W. Fischer, P. Meden, D. Krieger, K. Møller, G.M. Knudsen, L.H. Pinborg, In vivo quantification of cerebral translocator protein binding in humans using 6-chloro-2-(4'-¹²³I-iodophenyl)-3-(N,N-diethyl)-imidazo[1,2-a]pyridine-3-acetamide SPECT, *J. Nucl. Med.* 55 (2014) 1966–1972. doi:10.2967/jnumed.114.143727.
- [36] P. Jensen, L. Feng, I. Law, C. Svarer, G.M. Knudsen, J.D. Mikkelsen, R. de Nijs, V.A. Larsen, A. Dyssegaard, G. Thomsen, W. Fischer, D. Guilloteau, L.H. Pinborg, TSPO imaging in glioblastoma multiforme: a direct comparison between ¹²³I-CLINDE SPECT, ¹⁸F-FET PET, and gadolinium-enhanced MR imaging, *J. Nucl. Med.* 56 (2015) 1386–1390. doi:10.2967/jnumed.115.158998.
- [37] A. Colasanti, Q. Guo, P. Giannetti, M.B. Wall, R.D. Newbould, C. Bishop, M. Onega, R. Nicholas, O. Ciccarelli, P.A. Muraro, O. Malik, D.R. Owen, A.H. Young, R.N. Gunn, P. Piccini, P.M. Matthews, E.A. Rabiner, Hippocampal neuroinflammation, functional connectivity, and depressive symptoms in multiple sclerosis, *Biol. Psychiatry.* (n.d.). doi:10.1016/j.biopsych.2015.11.022.
- [38] S. Selleri, F. Bruni, C. Costagli, A. Costanzo, G. Guerrini, G. Ciciani, B. Costa, C. Martini, 2-Arylpyrazolo[1,5-a]pyrimidin-3-yl acetamides. New potent and selective peripheral benzodiazepine receptor ligands, *Bioorg. Med. Chem.* 9 (2001) 2661–2671. doi:10.1016/S0968-0896(01)00192-4.
- [39] A. Reynolds, R. Hanani, D. Hibbs, A. Damont, E.D. Pozzo, S. Selleri, F. Dollé, C. Martini, M. Kassiou, Pyrazolo[1,5-a]pyrimidine acetamides: 4-Phenyl alkyl ether derivatives as potent ligands for the 18kDa translocator protein (TSPO), *Bioorg. Med. Chem. Lett.* 20 (2010) 5799–5802. doi:10.1016/j.bmcl.2010.07.135.
- [40] S.D. Banister, S.M. Wilkinson, R. Hanani, A.J. Reynolds, D.E. Hibbs, M. Kassiou, A practical, multigram synthesis of the 2-(2-(4-alkoxyphenyl)-5,7-dimethylpyrazolo[1,5-a]pyrimidin-3-yl)acetamide (DPA) class of high affinity translocator protein (TSPO) ligands, *Tetrahedron Lett.* 53 (2012) 3780–3783. doi:10.1016/j.tetlet.2012.05.044.
- [41] S.D. Banister, C. Beinat, S.M. Wilkinson, B. Shen, C. Bartoli, S. Selleri, E. Da Pozzo, C. Martini, F.T. Chin, M. Kassiou, Ether analogues of DPA-714 with subnanomolar affinity for the translocator protein (TSPO), *Eur. J. Med. Chem.* 93 (2015) 392–400. doi:10.1016/j.ejmech.2015.02.004.
- [42] M.L. James, R.R. Fulton, D.J. Henderson, S. Eberl, S.R. Meikle, S. Thomson, R.D. Allan, F. Dollé, M.J. Fulham, M. Kassiou, Synthesis and in vivo evaluation of a novel peripheral benzodiazepine receptor PET radioligand, *Bioorg. Med. Chem.* 13 (2005) 6188–6194. doi:10.1016/j.bmc.2005.06.030.
- [43] C. Thominiaux, F. Dollé, M.L. James, Y. Bramoullé, H. Boutin, L. Besret, M.-C. Grégoire, H. Valette, M. Bottlaender, B. Tavitian, P. Hantraye, S. Selleri, M. Kassiou, Improved synthesis of the peripheral benzodiazepine receptor ligand [¹¹C]DPA-713 using [¹¹C]methyl triflate, *Appl. Radiat. Isot.* 64 (2006) 570–573. doi:10.1016/j.apradiso.2005.12.003.

- [44] M.L. James, R.R. Fulton, J. Vercoullie, D.J. Henderson, L. Garreau, S. Chalon, F. Dollé, S. Selleri, D. Guilloteau, M. Kassiou, DPA-714, a new translocator protein-specific ligand: synthesis, radiofluorination, and pharmacologic characterization, *J. Nucl. Med.* 49 (2008) 814–822. doi:10.2967/jnumed.107.046151.
- [45] A. Damont, F. Hinnen, B. Kuhnast, M.-A. Schöllhorn-Peyronneau, M. James, C. Luus, B. Tavitian, M. Kassiou, F. Dollé, Radiosynthesis of [18F]DPA-714, a selective radioligand for imaging the translocator protein (18 kDa) with PET, *J. Label. Compd. Radiopharm.* 51 (2008) 286–292. doi:10.1002/jlcr.1523.
- [46] B. Kuhnast, A. Damont, F. Hinnen, T. Catarina, S. Demphel, S. Le Helleix, C. Coulon, S. Goutal, P. Gervais, F. Dollé, [18F]DPA-714, [18F]PBR111 and [18F]FEDAA1106-selective radioligands for imaging TSPO 18 kDa with PET: automated radiosynthesis on a TRACERLab FX-FN synthesizer and quality controls, *Appl. Radiat. Isot.* 70 (2012) 489–497. doi:10.1016/j.apradiso.2011.10.015.
- [47] H. Boutin, F. Chauveau, C. Thominiaux, M.-C. Grégoire, M.L. James, R. Trebossen, P. Hantraye, F. Dollé, B. Tavitian, M. Kassiou, 11C-DPA-713: a novel peripheral benzodiazepine receptor PET ligand for in vivo imaging of neuroinflammation, *J. Nucl. Med.* 48 (2007) 573–581.
- [48] F. Chauveau, N.V. Camp, F. Dollé, B. Kuhnast, F. Hinnen, A. Damont, H. Boutin, M. James, M. Kassiou, B. Tavitian, Comparative evaluation of the translocator protein radioligands 11C-DPA-713, 18F-DPA-714, and 11C-PK11195 in a rat model of acute neuroinflammation, *J. Nucl. Med.* 50 (2009) 468–476. doi:10.2967/jnumed.108.058669.
- [49] J. Doorduyn, H.C. Klein, R.A. Dierckx, M. James, M. Kassiou, E.F.J. Vries, [11C]-DPA-713 and [18F]-DPA-714 as New PET Tracers for TSPO: A comparison with [11C]-(R)-PK11195 in a rat model of Herpes Encephalitis, *Mol. Imaging Biol.* 11 (2009) 386–398. doi:10.1007/s11307-009-0211-6.
- [50] C.J. Endres, J.M. Coughlin, K.L. Gage, C.C. Watkins, M. Kassiou, M.G. Pomper, Radiation dosimetry and biodistribution of the TSPO ligand 11C-DPA-713 in humans, *J. Nucl. Med.* 53 (2012) 330–335. doi:10.2967/jnumed.111.094565.
- [51] C.J. Endres, M.G. Pomper, M. James, O. Uzuner, D.A. Hammoud, C.C. Watkins, A. Reynolds, J. Hilton, R.F. Dannals, M. Kassiou, Initial evaluation of 11C-DPA-713, a novel TSPO PET ligand, in humans, *J. Nucl. Med.* 50 (2009) 1276–1282. doi:10.2967/jnumed.109.062265.
- [52] Gershen LD, Zanotti-Fregonara P, Dustin IH, et al, Neuroinflammation in temporal lobe epilepsy measured using positron emission tomographic imaging of translocator protein, *JAMA Neurol.* 72 (2015) 882–888. doi:10.1001/Neuro.2015.0941.
- [53] F. Chauveau, N.V. Camp, F. Dollé, B. Kuhnast, F. Hinnen, A. Damont, H. Boutin, M. James, M. Kassiou, B. Tavitian, Comparative evaluation of the Translocator Protein radioligands 11C-DPA-713, 18F-DPA-714, and 11C-PK11195 in a rat model of acute neuroinflammation, *J. Nucl. Med.* 50 (2009) 468–476. doi:10.2967/jnumed.108.058669.
- [54] D. Ory, A. Postnov, M. Koole, S. Celen, B. de Laat, A. Verbruggen, K.V. Laere, G. Bormans, C. Casteels, Quantification of TSPO overexpression in a rat model of local neuroinflammation induced by intracerebral injection of LPS by the use of [18F]DPA-714 PET, *Eur. J. Nucl. Med. Mol. Imaging.* 43 (2015) 163–172. doi:10.1007/s00259-015-3172-9.
- [55] S. Gargiulo, S. Anzilotti, A.R.D. Coda, M. Gramanzini, A. Greco, M. Panico, A. Vinciguerra, A. Zannetti, C. Vicidomini, F. Dollé, G. Pignataro, M. Quarantelli, L. Annunziato, A. Brunetti, M. Salvatore, S. Pappatà, Imaging of brain TSPO expression in a mouse model of amyotrophic lateral sclerosis with 18F-DPA-714 and micro-PET/CT, *Eur. J. Nucl. Med. Mol. Imaging.* 43 (2016) 1348–1359. doi:10.1007/s00259-016-3311-y.
- [56] C. Thomas, J. Vercoullie, A. Doméné, C. Tauber, M. Kassiou, D. Guilloteau, C. Destrieux, S. Sérrière, S. Chalon, Detection of neuroinflammation in a rat model of subarachnoid hemorrhage using [18F]DPA-714 PET imaging, *Mol. Imaging.* 15 (2016) 1–8. doi:10.1177/1536012116639189.

- [57] A. Martín, R. Boisgard, B. Thézé, N. Van Camp, B. Kuhnast, A. Damont, M. Kassiou, F. Dollé, B. Tavitian, Evaluation of the PBR/TSPO radioligand [18F]DPA-714 in a rat model of focal cerebral ischemia, *J. Cereb. Blood Flow Metab.* 30 (2010) 230–241. doi:10.1038/jcbfm.2009.205.
- [58] H. Boutin, C. Prenant, R. Maroy, J. Galea, A.D. Greenhalgh, A. Smigova, C. Cawthorne, P. Julyan, S.M. Wilkinson, S.D. Banister, G. Brown, K. Herholz, M. Kassiou, N.J. Rothwell, [18F]DPA-714: Direct comparison with [11C]PK11195 in a model of cerebral ischemia in rats, *PLOS ONE*. 8 (2013) e56441. doi:10.1371/journal.pone.0056441.
- [59] J. Zheng, A. Winkeler, M.-A. Peyronneau, F. Dollé, R. Boisgard, Evaluation of PET imaging performance of the TSPO radioligand [18F]DPA-714 in mouse and rat models of cancer and inflammation, *Mol. Imaging Biol.* 18 (2015) 127–134. doi:10.1007/s11307-015-0877-x.
- [60] A. Winkeler, R. Boisgard, A.R. Awde, A. Dubois, B. Thézé, J. Zheng, L. Ciobanu, F. Dollé, T. Viel, A.H. Jacobs, B. Tavitian, The translocator protein ligand [18F]DPA-714 images glioma and activated microglia in vivo, *Eur. J. Nucl. Med. Mol. Imaging.* 39 (2012) 811–823. doi:10.1007/s00259-011-2041-4.
- [61] G. Pottier, N. Bernards, F. Dollé, R. Boisgard, [¹⁸F]DPA-714 as a biomarker for positron emission tomography imaging of rheumatoid arthritis in an animal model, *Arthritis Res. Ther.* 16 (2014) R69. doi:10.1186/ar4508.
- [62] Y.Y.J. Gent, K. Weijers, C.F.M. Molthoff, A.D. Windhorst, M.C. Huisman, M. Kassiou, G. Jansen, A.A. Lammertsma, C.J. van der Laken, Promising potential of new generation translocator protein tracers providing enhanced contrast of arthritis imaging by positron emission tomography in a rat model of arthritis, *Arthritis Res. Ther.* 16 (2014) R70. doi:10.1186/ar4509.
- [63] N. Bernards, G. Pottier, B. Thézé, F. Dollé, R. Boisgard, In vivo evaluation of inflammatory bowel disease with the aid of μ PET and the translocator protein 18 kDa radioligand [18F]DPA-714, *Mol. Imaging Biol.* 17 (2015) 67–75. doi:10.1007/s11307-014-0765-9.
- [64] S. Lavissee, K. Inoue, C. Jan, M.A. Peyronneau, F. Petit, S. Goutal, J. Daugey, M. Guillermier, F. Dollé, L. Rbah-Vidal, N.V. Camp, R. Aron-Badin, P. Remy, P. Hantraye, [18F]DPA-714 PET imaging of translocator protein TSPO (18 kDa) in the normal and excitotoxically-lesioned nonhuman primate brain, *Eur. J. Nucl. Med. Mol. Imaging.* 42 (2014) 478–494. doi:10.1007/s00259-014-2962-9.
- [65] N. Arlicot, J. Vercouillie, M.-J. Ribeiro, C. Tauber, Y. Venel, J.-L. Baulieu, S. Maia, P. Corcia, M.G. Stabin, A. Reynolds, M. Kassiou, D. Guilloteau, Initial evaluation in healthy humans of [18F]DPA-714, a potential PET biomarker for neuroinflammation, *Nucl. Med. Biol.* 39 (2012) 570–578. doi:10.1016/j.nucmedbio.2011.10.012.
- [66] S. Lavissee, D. García-Lorenzo, M.-A. Peyronneau, B. Bodini, C. Thiriez, B. Kuhnast, C. Comtat, P. Remy, B. Stankoff, M. Bottlaender, Optimized quantification of translocator protein radioligand 18F-DPA-714 uptake in the brain of genotyped healthy volunteers, *J. Nucl. Med.* 56 (2015) 1048–1054. doi:10.2967/jnumed.115.156083.
- [67] S.S. Golla, R. Boellaard, V. Oikonen, A. Hoffmann, B.N.M. van Berckel, A.D. Windhorst, J. Virta, E.T. te Beek, G.J. Groeneveld, M. Haaparanta-Solin, P. Luoto, N. Savisto, O. Solin, R. Valencia, A. Thiele, J. Eriksson, R.C. Schuit, A.A. Lammertsma, J. Rinne, Parametric binding images of the TSPO ligand [18F]DPA-714, *J. Nucl. Med.* (2016) in press. doi:10.2967/jnumed.116.173013.
- [68] S.S.V. Golla, R. Boellaard, V. Oikonen, A. Hoffmann, B.N.M. van Berckel, A.D. Windhorst, J. Virta, M. Haaparanta-Solin, P. Luoto, N. Savisto, O. Solin, R. Valencia, A. Thiele, J. Eriksson, R.C. Schuit, A.A. Lammertsma, J.O. Rinne, Quantification of [18F]DPA-714 binding in the human brain: initial studies in healthy controls and Alzheimer's disease patients, *J. Cereb. Blood Flow Metab.* 35 (2015) 766–772. doi:10.1038/jcbfm.2014.261.
- [69] L. Hamelin, J. Lagarde, G. Dorothée, C. Leroy, M. Labit, R.A. Comley, L.C. de Souza, H. Corne, L. Dauphinot, M. Bertoux, B. Dubois, P. Gervais, O. Colliot, M.C. Potier, M. Bottlaender, M. Sarazin, Clinical IMABio3 team, Early and protective microglial

- activation in Alzheimer's disease: a prospective study using 18F-DPA-714 PET imaging, *Brain J. Neurol.* 139 (2016) 1252–1264. doi:10.1093/brain/aww017.
- [70] M.-J. Ribeiro, J. Vercouillie, S. Debiais, J.-P. Cottier, I. Bonnaud, V. Camus, S. Banister, M. Kassiou, N. Arlicot, D. Guilloteau, Could 18 F-DPA-714 PET imaging be interesting to use in the early post-stroke period?, *EJNMMI Res.* 4 (2014) 1–8. doi:10.1186/s13550-014-0028-4.
- [71] L. Pichard, G. Gillet, C. Bonfils, J. Domergue, J.P. Thénot, P. Maurel, Oxidative metabolism of zolpidem by human liver cytochrome P450S., *Drug Metab. Dispos.* 23 (1995) 1253–1262.
- [72] Garrigou-Gadenne, A. Durand, J.P. Thenot, P.L. Morselli, The disposition and pharmacokinetics of alpidem, a new anxiolytic, in the rat., *Drug Metab. Dispos.* 19 (1991) 574–579.
- [73] A. Katsifis, C. Loc'h, D. Henderson, T. Bourdier, T. Pham, I. Greguric, P. Lam, P. Callaghan, F. Mattner, S. Eberl, M. Fulham, A rapid solid-phase extraction method for measurement of non-metabolised peripheral benzodiazepine receptor ligands, [18F]PBR102 and [18F]PBR111, in rat and primate plasma, *Nucl. Med. Biol.* 38 (2011) 137–148. doi:10.1016/j.nucmedbio.2010.07.008.
- [74] M.-A. Peyronneau, W. Saba, S. Goutal, A. Damont, F. Dollé, M. Kassiou, M. Bottlaender, H. Valette, Metabolism and quantification of [18F]DPA-714, a new TSPO Positron Emission Tomography radioligand, *Drug Metab. Dispos.* 41 (2013) 122–131. doi:10.1124/dmd.112.046342.
- [75] V. Médran-Navarrete, A. Damont, M.-A. Peyronneau, B. Kuhnast, N. Bernards, G. Pottier, F. Marguet, F. Puech, R. Boisgard, F. Dollé, Preparation and evaluation of novel pyrazolo[1,5-a]pyrimidine acetamides, closely related to DPA-714, as potent ligands for imaging the TSPO 18 kDa with PET, *Bioorg. Med. Chem. Lett.* 24 (2014) 1550–1556. doi:10.1016/j.bmcl.2014.01.080.
- [76] A. Damont, V. Médran-Navarrete, F. Cacheux, B. Kuhnast, G. Pottier, N. Bernards, F. Marguet, F. Puech, R. Boisgard, F. Dollé, Novel pyrazolo[1,5-a]pyrimidines as translocator protein 18 kDa (TSPO) ligands: synthesis, in vitro biological evaluation, [18F]-labeling, and in vivo neuroinflammation PET images, *J. Med. Chem.* 58 (2015) 7449–7464. doi:10.1021/acs.jmedchem.5b00932.
- [77] D.R. Sidler, T.C. Lovelace, J.M. McNamara, P.J. Reider, Aluminum-amine complexes for the conversion of carboxylic esters to amides. Application to the synthesis of LTD4 antagonist MK-0679, *J. Org. Chem.* 59 (1994) 1231–1233. doi:10.1021/jo00085a001.
- [78] A. Basha, M. Lipton, S.M. Weinreb, A mild, general method for conversion of esters to amides, *Tetrahedron Lett.* 18 (1977) 4171–4172. doi:10.1016/S0040-4039(01)83457-2.
- [79] J.I. Levin, E. Tuross, S.M. Weinreb, An alternative procedure for the aluminum-mediated conversion of esters to amides, *Synth. Commun.* 12 (1982) 989–993. doi:10.1080/00397918208061938.
- [80] K. Yoshida, K. Nakayama, Y. Yokomizo, M. Ohtsuka, M. Takemura, K. Hoshino, H. Kanda, K. Namba, H. Nitani, J.Z. Zhang, V.J. Lee, W.J. Watkins, MexAB-OprM specific efflux pump inhibitors in *Pseudomonas aeruginosa*. Part 6: Exploration of aromatic substituents, *Bioorg. Med. Chem.* 14 (2006) 8506–8518. doi:10.1016/j.bmc.2006.08.037.
- [81] E. Barresi, A. Bruno, S. Taliani, S. Cosconati, E. Da Pozzo, S. Salerno, F. Simorini, S. Daniele, C. Giacomelli, A.M. Marini, C. La Motta, L. Marinelli, B. Cosimelli, E. Novellino, G. Greco, F. Da Settimo, C. Martini, Deepening the topology of the translocator protein binding site by novel N,N-dialkyl-2-arylidol-3-ylglyoxylamides, *J. Med. Chem.* 58 (2015) 6081–6092. doi:10.1021/acs.jmedchem.5b00689.
- [82] G. Trapani, M. Franco, L. Ricciardi, A. Latrofa, G. Genchi, E. Sanna, F. Tuveri, E. Cagetti, G. Biggio, G. Liso, Synthesis and binding affinity of 2-phenylimidazo [1, 2-a] pyridine derivatives for both central and peripheral benzodiazepine receptors. A new series of high-affinity and selective ligands for the peripheral type, *J. Med. Chem.* 40 (1997) 3109–3118.

- [83] G. Trapani, M. Franco, A. Latrofa, A. Carotti, M. Serra, E. Sanna, G. Biggio, G. Liso, Novel 2-phenylimidazo[1,2-*a*]pyridine derivatives as potent and selective ligands for Peripheral Benzodiazepine Receptors: Synthesis, binding affinity, and in vivo studies, *J. Med. Chem.* 42 (1999) 3934–3941. doi:10.1021/jm991035g.
- [84] G. Trapani, V. Laquintana, N. Denora, A. Trapani, A. Lopodota, A. Latrofa, M. Franco, M. Serra, M.G. Pisu, I. Floris, E. Sanna, G. Biggio, G. Liso, Structure–activity relationships and effects on neuroactive steroid synthesis in a series of 2-phenylimidazo[1,2-*a*]pyridineacetamide Peripheral Benzodiazepine Receptors ligands, *J. Med. Chem.* 48 (2005) 292–305. doi:10.1021/jm049610q.
- [85] S.A. Hithcock, L.D. Pennington, Structure-brain exposure relationships, *J. Med. Chem.* 49 (2006) 7559–7583. doi:10.1021/jm0606642i.